UNIVERSIDAD DE CONCEPCIÓN

Centro de Investigación en
Ingeniería Matemática (CI^{2}MA)

A posteriori error analysis of a mixed-primal finite element method for the Boussinesq problem with temperature-dependant viscosity

Javier A. Almonacid, Gabriel N. Gatica,
Ricardo Oyarzúa

PREPRINT 2018-07

SERIE DE PRE-PUBLICACIONES

A posteriori error analysis of a mixed-primal finite element method for the Boussinesq problem with temperature-dependant viscosity*

Javier A. Almonacid† Gabriel N. Gatica‡ Ricardo Oyarzúa§

Abstract

We have recently proposed a new finite element method for a more general Boussinesq model in 2D given by the case in which the viscosity of the fluid depends on its temperature. Our approach is based on a pseudostress-velocity-vorticity mixed formulation for the momentum equations, which is suitably augmented with Galerkin-type terms, coupled with the usual primal formulation for the energy equation, along with the introduction of the normal heat flux on the boundary as a Lagrange multiplier taking care of the fact that the prescribed temperature there becomes an essential condition. Then, fixed-point arguments using Banach and Brouwer theorems, in addition to other classical tools from functional and numerical analysis, provide sufficient conditions ensuring well-posedness of the resulting continuous and discrete sytems, together with the corresponding error estimates and associated rates of convergence. In the present work we complement these results with the derivation of a reliable and efficient residual-based a posteriori error estimator for the aforementioned augmented mixed-primal finite element method. Duality techniques, Helmholtz decompositions, and the approximation properties of the Raviart-Thomas and Clément interpolants are applied to obtain a reliable global error indicator. In turn, standard tools including the usual localization technique of bubble functions and inverse inequalities, and a regularity assumption originally utilized in the previous well-posedness and a priori error analyses, are employed to prove its efficiency. Finally, a reliable fully local and computable a posteriori error estimator induced by the aforementioned one is deduced, and several numerical results illustrating its performance and validating the expected behaviour of the associated adaptive algorithm are reported.

Key words: Boussinesq model, augmented mixed–primal formulation, a posteriori error analysis, reliability, efficiency, adaptive algorithm.

Mathematics subject classifications (2000): 65N30, 65N12, 65N15, 35Q79, 80A20, 76R05, 76D07

1 Introduction

A wide variety of natural convection flows can be modelled using the equations of conservation of mass, momentum and energy, coupled by means of the Boussinesq approximation, in what we refer to as the Boussinesq problem. In recent work [1], we have analyzed the problem considering a fluid with

*This work was partially supported by CONICYT-Chile through BASAL project CMM, Universidad de Chile, and Fondecyt project 1161325; and by Centro de Investigación en Ingeniería Matemática (CI^{2}MA), Universidad de Concepción.

†Centro de Investigación en Ingeniería Matemática (CI^{2}MA), Universidad de Concepción, Casilla 160-C, Concepción, Chile, email: jalmonacid@ci2ma.udec.cl.

‡CI^{2}MA and Departamento de Ingeniería Matemática, Universidad de Concepción, Casilla 160-C, Concepción, Chile, email: ggatica@ci2ma.udec.cl.

§GIMNAP-Departamento de Matemática, Universidad del Bío-Bío, Casilla 5-C, Concepción, Chile, and CI^{2}MA, Universidad de Concepción, Casilla 160-C, Concepción, Chile, email: royarzua@ubiobio.cl.

a temperature-dependent viscosity and a tensorial thermal conductivity, which leaded us to construct an augmented mixed-primal finite element method that approximates the pseudostress tensor using Raviart-Thomas elements of order $k+1$, the velocity and temperature with Lagrange elements of order k, and the vorticity tensor and normal heat flux on the boundary with discontinuous piecewise polynomials of degree $\leq k$, thus obtaining optimal *a priori* bounds under smooth enough solutions. However, it is expected from the literature (see, e.g., [20, 21]) that, in the presence of singularities or high gradients, these rates of convergence will not be optimal, mainly because of the high degree of mesh refinement needed to capture those zones. Therefore, it is highly advisable the utilization of an *a posteriori* error estimator that measures the error in these particular areas, to then use an adaptive algorithm that decreases the computational cost of computing the solution on a highly refined mesh.

In this regard, several error estimators have been proposed in the context of the Boussinesq problems with constant viscosity and coupled problems in fluid mechanics with varying viscosity (see, e.g., [2, 6, 9, 12, 22]). On the one hand, the authors in [2] propose an *a posteriori* error estimator for a coupled-flow transport problem based on a Stokes-type equation, in which the viscosity depends on the gradient of the concentration, and a convection-diffusion equation with varying parameters. This was later on extended in [3] to a sedimentation-consolidation system, in which the aforementioned dependence for the viscosity of the fluid reduces just to the concentration itself instead of its gradient. On the other hand, the authors in [9] and [10] construct *a posteriori* error estimators for mixed-primal and fully-mixed formulations, respectively, of the Boussinesq problem with constant viscosity. All these works utilize duality arguments and Helmholtz decompositions to prove the reliability of the residual-based estimator, and inverse inequalities and localization arguments to obtain the efficiency estimates.

According to the above, it is the purpose of this paper to develop a reliable and efficient residual-based *a posteriori* error estimator (together with a fully-local version that can be used in an adaptive procedure) for the Boussinesq problem with temperature-dependent viscosity in the pseudostress-vorticity–based formulation from [1]. As a framework to begin the analysis, we consider the steps given by the authors in [2] and [9], previously mentioned in the foregoing paragraph. More precisely, inf-sup conditions coming from the well-posedness of the momentum and energy equations will give us a first sight of the estimator, then, the reliability of the estimator is proved using properties of the Raviart-Thomas and Clément interpolation operators, together with a Helmholtz decomposition of the space the pseudostress belongs to. Then, some inverse inequalities from [16], a localization technique based on bubble functions used in [9], and further-regularity assumptions on the solution to the momentum equation that were already used in the analysis of [1] will serve to prove the efficiency of the estimator. In addition, a fully local version is developed based on interpolation arguments and several numerical tests are realized where it can be seen that this new estimator is not only reliable (as proved theoretically) but also efficient, and it is capable to capture zones with high gradients and nearby singularities. We remark in advance that the uncoupling of the equations of momentum and energy allows us to reuse the results derived in [9] for the last one, which we will only cite, unless substantial differences appear.

1.1 Outline

The remainder of this paper is organized as follows. We end this section with some notation used throughout this work. Then, in Section 2, we recall the model problem from [1] and basic assumptions on the provided data, along with well-posedness results of the continuous and discrete formulations. Next, in Section 3, we introduce a residual-based *a posteriori* error estimator that is proved to be reliable and efficient, though the presence of a non-local term makes it inadvisable for adaptivity purposes. To remediate this, a fully-local version of the estimator is derived, to then, in Section 4, present a series of numerical examples that show its good performance and its behaviour upon an adaptive refinement technique.

1.2 Notation

Let us denote by $\Omega \subset \mathrm{R}^2$ a given bounded domain with polyhedral boundary Γ, and denote by $\boldsymbol{\nu}$ the outward unit normal vector on Γ. Standard notation will be adopted for Lebesgue spaces $\mathrm{L}^p(\Omega)$ and Sobolev spaces $\mathrm{W}^{s,2}(\Omega) =: \mathrm{H}^s(\Omega)$ with norm $\|\cdot\|_{s,\Omega}$ and seminorm $|\cdot|_{s,\Omega}$. In particular, $\mathrm{H}^{1/2}(\Gamma)$ is the space of traces of functions in $\mathrm{H}^1(\Omega)$ and $\mathrm{H}^{-1/2}(\Gamma)$ denotes its dual. By $\mathbf{M}$ and $\mathbb{M}$ we will denote the corresponding vectorial and tensorial counterparts of the generic scalar functional space M, and $\|\cdot\|$, with no subscripts, will stand for the natural norm of either an element or an operator in any product functional space. In turn, for any vector fields $\mathbf{v} = (v_i)_{i=1,2}$ and $\mathbf{w} = (w_i)_{i=1,2}$, we set the gradient, divergence and tensor product operators, as

$$\nabla \mathbf{v} := \left(\frac{\partial v_i}{\partial x_j}\right)_{i,j=1,2}, \quad \operatorname{div} \mathbf{v} := \sum_{j=1}^{2} \frac{\partial v_j}{\partial x_j}, \quad \text{and} \quad \mathbf{v} \otimes \mathbf{w} := (v_i w_j)_{i,j=1,2}.$$

In addition, for any tensor fields $\boldsymbol{\tau} = (\tau_{ij})_{i,j=1,2}$ and $\boldsymbol{\zeta} = (\zeta_{ij})_{i,j=1,2}$, we let $\mathbf{div}\,\boldsymbol{\tau}$ be the divergence operator div acting along the rows of $\boldsymbol{\tau}$, and define the transpose, the trace, the tensor inner product, and the deviatoric tensor, respectively, as

$$\boldsymbol{\tau}^{\mathtt{t}} := (\tau_{ji})_{i,j=1,2}, \quad \operatorname{tr}(\boldsymbol{\tau}) := \sum_{i=1}^{2} \tau_{ii}, \quad \boldsymbol{\tau} : \boldsymbol{\zeta} := \sum_{i,j=1}^{2} \tau_{ij}\zeta_{ij}, \quad \text{and} \quad \boldsymbol{\tau}^{\mathtt{d}} := \boldsymbol{\tau} - \frac{1}{2}\operatorname{tr}(\boldsymbol{\tau})\mathbb{I},$$

where $\mathbb{I}$ stands for the identity tensor in $\mathbb{R} := \mathrm{R}^{2\times 2}$. Furthermore, we recall that

$$\mathbb{H}(\mathbf{div};\Omega) := \left\{\boldsymbol{\tau} \in \mathbb{L}^2(\Omega) : \mathbf{div}\,\boldsymbol{\tau} \in \mathbf{L}^2(\Omega)\right\},$$

equipped with the usual norm

$$\|\boldsymbol{\tau}\|^2_{\mathbf{div};\Omega} := \|\boldsymbol{\tau}\|^2_{0,\Omega} + \|\mathbf{div}\,\boldsymbol{\tau}\|^2_{0,\Omega},$$

is a standard Hilbert space in the realm of mixed problems. Finally, in what follows, $|\cdot|$ denotes the Euclidean norm in $\mathbf{R} := \mathrm{R}^2$. Also, we employ $\mathbf{0}$ to denote a generic null vector and use C, with or without subscripts, bars, tildes or hats, to mean generic positive constants independent of the discretization parameters, which may take different values at different places.

2 The Boussinesq problem

We now recall the Boussinesq problem in the pseudostress-vorticity–based formulation considered in [1], to then cite some key results about the augmented mixed-primal finite element method developed in it.

2.1 The mathematical model

Let $\mathbf{u}$, p and φ be the velocity, pressure and temperature, respectively, of a non-isothermal, incompressible, Newtonian fluid whose transversal section occupies the two-dimensional region Ω with polygonal boundary Γ. Then, neglecting the presence of source terms in the equilibrium equations, the Boussinesq problem can be written as

$$
\begin{aligned}
-\mathbf{div}\,(\mu(\varphi)\mathbf{e}(\mathbf{u})) + (\nabla\mathbf{u})\mathbf{u} + \nabla p - \varphi\mathbf{g} &= 0 \quad \text{in } \Omega\,, && (2.1a)\\
\operatorname{div}\mathbf{u} &= 0 \quad \text{in } \Omega\,, && (2.1b)\\
-\operatorname{div}(\mathbb{K}\nabla\varphi) + \mathbf{u}\cdot\nabla\varphi &= 0 \quad \text{in } \Omega\,, && (2.1c)\\
\mathbf{u} &= \mathbf{u}_D \quad \text{on } \Gamma\,, && (2.1d)\\
\varphi &= \varphi_D \quad \text{on } \Gamma\,, && (2.1e)
\end{aligned}
$$

where $\mathbf{e}(\mathbf{u})$ is the symmetric part of the velocity gradient tensor $\nabla\mathbf{u}$, μ denotes the viscosity of the fluid (that may depend on its temperature φ), $\mathbb{K}$ is the thermal conductivity tensor and $-\mathbf{g}$ is a body force per unit mass. The reader may refer to [7] for further details concerning the theoretical aspects of this fluid mechanics topic, as well as the derivation of the equations.

In what follows, we assume $\mu : \mathrm{R} \to \mathrm{R}^+$ to be a bounded, Lipschitz continuous, and continuously differentiable function, that is, $\mu \in C^1(\mathrm{R})$ and there exist positive constants μ_1, μ_2, L_μ such that

$$
\mu_1 \leq \mu(t) \leq \mu_2 \quad \text{and} \quad |\mu(s) - \mu(t)| \leq L_\mu |s-t| \quad \forall\, s,t \in R. \tag{2.2}
$$

In addition, we suppose that $\mathbb{K} \in \mathbb{L}^\infty(\Omega)$, $\mathbf{g} \in \mathbf{L}^\infty(\Omega)$, $\mathbf{u}_D \in \mathbf{H}^{1/2}(\Gamma)$, $\varphi_D \in \mathrm{H}^{1/2}(\Gamma)$ and that $\mathbf{u}_D$ verifies the compatibility condition

$$
\int_\Gamma \mathbf{u}_D \cdot \boldsymbol{\nu} = 0. \tag{2.3}
$$

2.2 A pseudostress-vorticity–based formulation

Let $\boldsymbol{\sigma}$ and $\boldsymbol{\gamma}$ be the pseudostress and vorticity tensors, respectively defined as

$$
\boldsymbol{\sigma} := \mu(\varphi)\mathbf{e}(\mathbf{u}) - \mathbf{u}\otimes\mathbf{u} - p\mathbb{I} \quad \text{and} \quad \boldsymbol{\gamma} := \boldsymbol{\omega}(\mathbf{u}), \tag{2.4}
$$

where $\boldsymbol{\omega}(\mathbf{u})$ is the skew-symmetric part of the velocity gradient tensor $\nabla\mathbf{u}$, that is, for any velocity $\mathbf{v}$,

$$
\boldsymbol{\omega}(\mathbf{v}) := \frac{1}{2}\Big\{\nabla\mathbf{v} - (\nabla\mathbf{v})^{\mathtt{t}}\Big\}.
$$

Then, we denote by $\mathbb{L}^2_{\mathtt{skew}}(\Omega)$ the space of skew-symmetric tensors with components in $\mathrm{L}^2(\Omega)$, that is,

$$
\mathbb{L}^2_{\mathtt{skew}}(\Omega) := \Big\{\boldsymbol{\eta} \in \mathbb{L}^2(\Omega) : \boldsymbol{\eta} + \boldsymbol{\eta}^{\mathtt{t}} = \mathbf{0}\Big\}.
$$

Hence, (2.1) can be rewritten as: Find $(\boldsymbol{\sigma}, \mathbf{u}, \boldsymbol{\gamma}, \varphi)$ such that

$$
\begin{aligned}
\nabla\mathbf{u} - \boldsymbol{\gamma} - \frac{1}{\mu(\varphi)}\,(\mathbf{u}\otimes\mathbf{u})^{\mathtt{d}} &= \frac{1}{\mu(\varphi)}\,\boldsymbol{\sigma}^{\mathtt{d}} \quad \text{in } \Omega, && (2.5a)\\
-\mathbf{div}\,\boldsymbol{\sigma} - \varphi\mathbf{g} &= 0 \quad \text{in } \Omega, && (2.5b)\\
-\operatorname{div}(\mathbb{K}\nabla\varphi) + \mathbf{u}\cdot\nabla\varphi &= 0 \quad \text{in } \Omega, && (2.5c)\\
\mathbf{u} &= \mathbf{u}_D \quad \text{on } \Gamma, && (2.5d)\\
\varphi &= \varphi_D \quad \text{on } \Gamma, && (2.5e)\\
\int_\Omega \operatorname{tr}(\boldsymbol{\sigma} + \mathbf{u}\otimes\mathbf{u}) &= 0\,, && (2.5f)
\end{aligned}
$$

where the pressure p is postprocessed by means of the formula

$$
p = -\frac{1}{2}\operatorname{tr}\Big(\boldsymbol{\sigma} + \mathbf{u}\otimes\mathbf{u}\Big),
$$

and its uniqueness is ensured with (2.5f), for it implies that p has zero mean-value in Ω.

2.3 The augmented mixed-primal formulation

The construction of a weak formulation for (2.5) relies on the orthogonal decomposition

$$\mathbb{H}(\mathbf{div};\Omega) = \mathbb{H}_0(\mathbf{div};\Omega) \oplus \mathrm{R}\mathbb{I},$$

where

$$\mathbb{H}_0(\mathbf{div};\Omega) := \left\{ \boldsymbol{\zeta} \in \mathbb{H}(\mathbf{div};\Omega) : \int_\Omega \mathrm{tr}(\boldsymbol{\zeta}) = 0 \right\},$$

since it can be proved that the uniqueness condition (2.5f) allows us to only search for the $\mathbb{H}_0(\mathbf{div};\Omega)$-component of the pseudostress (cf. [1, Lemma 3.1]). In addition, the mixed formulation for the momentum equation is augmented with Galerkin-type terms, thus allowing a proper analysis of the weak problem, and ensuring also conformity in the scheme, since at a first glance the velocity lives in $\mathbf{H}^1(\Omega)$, whereas its test function lives in $\mathbf{L}^2(\Omega)$. On the other hand, a primal formulation for the energy equations leads us to define the Lagrange multiplier on Γ (known as the normal heat flux)

$$\lambda := -\mathbb{K}\nabla\varphi \cdot \boldsymbol{\nu} \in \mathrm{H}^{-1/2}(\Gamma),$$

and to weakly impose the prescribed temperature on the boundary. Therefore, denoting $\vec{\boldsymbol{\sigma}}, \vec{\boldsymbol{\tau}} \in \mathbb{H}_0(\mathbf{div};\Omega) \times \mathbf{H}^1(\Omega) \times \mathbb{L}^2_{\mathtt{skew}}(\Omega)$ by

$$\vec{\boldsymbol{\sigma}} := (\boldsymbol{\sigma}, \mathbf{u}, \boldsymbol{\gamma}), \quad \vec{\boldsymbol{\tau}} := (\boldsymbol{\tau}, \mathbf{v}, \boldsymbol{\eta}),$$

the augmented mixed-primal formulation reads: Find $(\vec{\boldsymbol{\sigma}}, (\varphi, \lambda)) \in \mathbb{H}_0(\mathbf{div};\Omega) \times \mathbf{H}^1(\Omega) \times \mathbb{L}^2_{\mathtt{skew}}(\Omega) \times \mathrm{H}^1(\Omega) \times \mathrm{H}^{-1/2}(\Gamma)$ such that

$$\mathbf{A}_\varphi(\vec{\boldsymbol{\sigma}}, \vec{\boldsymbol{\tau}}) + \mathbf{B}_{\mathbf{u},\varphi}(\vec{\boldsymbol{\sigma}}, \vec{\boldsymbol{\tau}}) = F_\varphi(\vec{\boldsymbol{\tau}}) + F_D(\vec{\boldsymbol{\tau}}), \tag{2.6a}$$

$$\mathbf{a}(\varphi, \psi) + \mathbf{b}(\psi, \lambda) = F_{\mathbf{u},\varphi}(\psi), \tag{2.6b}$$

$$\mathbf{b}(\varphi, \xi) = G(\xi), \tag{2.6c}$$

for all $(\vec{\boldsymbol{\tau}}, (\psi, \xi)) \in \mathbb{H}_0(\mathbf{div};\Omega) \times \mathbf{H}^1(\Omega) \times \mathbb{L}^2_{\mathtt{skew}}(\Omega) \times \mathrm{H}^1(\Omega) \times \mathrm{H}^{-1/2}(\Gamma)$, where given positive stabilization parameters κ_i, $i \in \{1,2,3,4\}$ and a pair $(\mathbf{w}, \phi) \in \mathbf{H}^1(\Omega) \times \mathrm{H}^1(\Omega)$, the bounded bilinear forms $\mathbf{A}_\phi$, $\mathbf{B}_{\mathbf{w},\phi}$, $\mathbf{a}$ and $\mathbf{b}$; and the functionals F_D, F_ϕ, $F_{\mathbf{w},\phi}$ and G are defined as

$$\begin{aligned}\mathbf{A}_\phi(\vec{\boldsymbol{\sigma}}, \vec{\boldsymbol{\tau}}) := & \int_\Omega \frac{1}{\mu(\phi)} \boldsymbol{\sigma}^{\mathrm{d}} : \left\{ \boldsymbol{\tau}^{\mathrm{d}} - \kappa_1 \mathbf{e}(\mathbf{v}) \right\} + \int_\Omega \left\{ \mathbf{u} + \kappa_2 \mathbf{div}\,\boldsymbol{\sigma} \right\} \cdot \mathbf{div}\,\boldsymbol{\tau} + \kappa_1 \int_\Omega \mathbf{e}(\mathbf{u}) : \mathbf{e}(\mathbf{v}) \\ & + \int_\Omega \boldsymbol{\gamma} : \boldsymbol{\tau} - \int_\Omega \mathbf{v} \cdot \mathbf{div}\,\boldsymbol{\sigma} - \int_\Omega \boldsymbol{\sigma} : \boldsymbol{\eta} + \kappa_3 \int_\Omega \left\{ \boldsymbol{\gamma} - \boldsymbol{\omega}(\mathbf{u}) \right\} : \boldsymbol{\eta} + \kappa_4 \int_\Gamma \mathbf{u} \cdot \mathbf{v},\end{aligned} \tag{2.7}$$

$$\mathbf{B}_{\mathbf{w},\phi}(\vec{\boldsymbol{\sigma}}, \vec{\boldsymbol{\tau}}) := \int_\Omega \frac{1}{\mu(\phi)} (\mathbf{u} \otimes \mathbf{w})^{\mathrm{d}} : \left\{ \boldsymbol{\tau}^{\mathrm{d}} - \kappa_1 \mathbf{e}(\mathbf{v}) \right\}, \tag{2.8}$$

for all $\vec{\boldsymbol{\sigma}}, \vec{\boldsymbol{\tau}} \in \mathbb{H}_0(\mathbf{div};\Omega) \times \mathbf{H}^1(\Omega) \times \mathbb{L}^2_{\mathtt{skew}}(\Omega)$;

$$\mathbf{a}(\varphi, \psi) := \int_\Omega \mathbb{K}\nabla\varphi \cdot \nabla\psi, \tag{2.9}$$

for all $\varphi, \psi \in \mathrm{H}^1(\Omega)$;

$$\mathbf{b}(\psi, \xi) := \langle \xi, \psi \rangle_\Gamma, \tag{2.10}$$

for all $(\psi, \xi) \in \mathrm{H}^1(\Omega) \times \mathrm{H}^{-1/2}(\Gamma)$;

$$F_D(\vec{\boldsymbol{\tau}}) := \langle \boldsymbol{\tau}\boldsymbol{\nu}, \mathbf{u}_D \rangle_\Gamma + \kappa_4 \int_\Gamma \mathbf{u}_D \cdot \mathbf{v}, \tag{2.11}$$

$$F_\phi(\vec{\boldsymbol{\tau}}) := \int_\Omega \phi\mathbf{g}\cdot\Big\{\mathbf{v} - \kappa_2\mathbf{div}\,\boldsymbol{\tau}\Big\}, \tag{2.12}$$

for all $\vec{\boldsymbol{\tau}} \in \mathbb{H}_0(\mathbf{div};\Omega)\times\mathbf{H}^1(\Omega)\times\mathbb{L}^2_{\mathtt{skew}}(\Omega)$;

$$F_{\mathbf{w},\phi}(\psi) = -\int_\Omega \psi\mathbf{u}\cdot\nabla\phi, \tag{2.13}$$

for all $\psi \in \mathrm{H}^1(\Omega)$; and

$$G(\xi) = \langle\, \xi, \varphi_D \,\rangle_\Gamma, \tag{2.14}$$

for all $\xi \in \mathrm{H}^{-1/2}(\Gamma)$.

This problem is analysed throughout [1, Section 3], and the well-posedness comes as a result of the application of a decoupling technique and a fixed-point strategy. Hence, assuming that the mixed formulation of the momentum equation has a slightly more regular solution, and the data is sufficiently small, it is possible to prove that for certain positive values of κ_i, $i \in \{1,2,3,4\}$, and for a suitable choosen constant $r_0 > 0$, there exists a unique solution $(\vec{\boldsymbol{\sigma}},(\varphi,\lambda)) \in \mathbb{H}_0(\mathbf{div};\Omega)\times\mathbf{H}^1(\Omega)\times\mathbb{L}^2_{\mathtt{skew}}(\Omega)\times \mathrm{H}^1(\Omega)\times\mathrm{H}^{-1/2}(\Gamma)$, with $(\mathbf{u},\varphi) \in W := \Big\{(\mathbf{w},\phi)\in\mathbf{H}^1(\Omega)\times\mathrm{H}^1(\Omega) : \|\,(\mathbf{w},\phi)\,\| \le r\Big\}$, $r \in (0, r_0)$ (cf. [1, Theorem 3.11]) such that there hold

$$\|\,\vec{\boldsymbol{\sigma}}\,\| \le C_{\mathbf{S}}\Big\{r\|\,\mathbf{g}\,\|_{\infty,\Omega} + \|\,\mathbf{u}_D\,\|_{1/2,\Gamma} + \|\,\mathbf{u}_D\,\|_{0,\Gamma}\Big\} \tag{2.15}$$

and

$$\|\,(\varphi,\lambda)\,\| \le C_{\widetilde{\mathbf{S}}}\Big\{r\|\,\mathbf{u}\,\|_{1,\Omega} + \|\,\varphi_D\,\|_{1/2,\Gamma}\Big\}, \tag{2.16}$$

where $C_{\mathbf{S}}$ and $C_{\widetilde{\mathbf{S}}}$ are positive constants.

2.4 The augmented mixed-primal finite element method

Let $\{\mathcal{T}_h\}_{h>0}$ be a family of regular triangulations of $\overline{\Omega}$, each of them made of triangles T of diameter h_T and define the global mesh size $h := \max_{T\in\mathcal{T}_h} h_T$. Given also $k \ge 0$, for each $T \in \mathcal{T}_h$ we let $P_k(T)$ be the space of polynomial functions on T of degree $\le k$ and denote by $\mathbb{RT}_k(T)$ the tensor version of the local Raviart-Thomas space of order k. In turn, we introduce the corresponding global Raviart-Thomas space

$$\mathbb{RT}_k(\mathcal{T}_h) \,:\, \Big\{\boldsymbol{\tau}\in\mathbb{H}(\mathbf{div};\Omega) : \quad \boldsymbol{\tau}|_T \in \mathbb{RT}_k(T) \quad \forall\, T\in\mathcal{T}_h\Big\}.$$

Thus, we consider the following finite element spaces to approximate respectively the pseudostress, velocity and vorticity variables:

$$\mathbb{H}_h^{\boldsymbol{\sigma}} := \mathbb{H}_0(\mathbf{div};\Omega) \cap \mathbb{RT}_k(\mathcal{T}_h)\,, \tag{2.17}$$

$$\mathbf{H}_h^{\mathbf{u}} := \big\{\mathbf{v}_h \in \mathbf{C}(\bar{\Omega}) : \quad \mathbf{v}_h\big|_T \in \mathbf{P}_{k+1}(T), \quad \forall\, T\in\mathcal{T}_h\big\}\,, \tag{2.18}$$

$$\mathbb{H}_h^{\boldsymbol{\gamma}} := \big\{\boldsymbol{\eta}_h \in \mathbb{L}^2_{\mathtt{skew}}(\Omega) : \quad \boldsymbol{\eta}_h\big|_T \in \mathbb{P}_k(T), \quad \forall\, T\in\mathcal{T}_h\big\}\,, \tag{2.19}$$

this is, finite element spaces of Raviart-Thomas of order k for $\boldsymbol{\sigma}$, Lagrange of order $k+1$ for $\mathbf{u}$, and piecewise skew-symmetric polynomial tensors of degree $\le k$ for $\boldsymbol{\gamma}$. On the other hand, the temperature φ is approximated using a Lagrange finite element space of order $k+1$,

$$\mathrm{H}_h^{\varphi} := \big\{\psi_h \in C(\bar{\Omega}) : \quad \psi_h\big|_T \in P_{k+1}(T), \quad \forall\, T\in\mathcal{T}_h\big\}\,, \tag{2.20}$$

and for the normal heat flux λ, we let $\{\widetilde{\Gamma}_1,\widetilde{\Gamma}_2,\ldots,\widetilde{\Gamma}_m\}$ be an independent triangulation of Γ (made of straight segments), and define $\widetilde{h} := \max_{j\in\{1,\ldots,m\}} |\widetilde{\Gamma}_j|$. Then, with the same integer $k \ge 0$ used in definitions (2.17), (2.18), (2.19), we approximate λ by piecewise polynomials of degree $\leq k$ over this new mesh, that is

$$\mathrm{H}^{\lambda}_{\widetilde{h}} := \left\{ \xi_{\widetilde{h}} \in \mathrm{L}^2(\Gamma) : \quad \xi_{\widetilde{h}}\big|_{\widetilde{\Gamma}_j} \in P_k(\widetilde{\Gamma}_j) \quad \forall\, j \in \{1, \dots, m\} \right\}. \tag{2.21}$$

In this way, the augmented mixed-primal finite element method reads: Find $(\vec{\boldsymbol{\sigma}}_h, (\varphi_h, \lambda_{\widetilde{h}})) \in \mathbb{H}^{\boldsymbol{\sigma}}_h \times \mathbf{H}^{\mathbf{u}}_h \times \mathbb{H}^{\gamma}_h \times \mathrm{H}^{\varphi}_h \times \mathrm{H}^{\lambda}_{\widetilde{h}}$ such that

$$\mathbf{A}_{\varphi_h}(\vec{\boldsymbol{\sigma}}_h, \vec{\boldsymbol{\tau}}_h) + \mathbf{B}_{\mathbf{u}_h,\varphi_h}(\vec{\boldsymbol{\sigma}}_h, \vec{\boldsymbol{\tau}}_h) = F_{\varphi_h}(\vec{\boldsymbol{\tau}}_h) + F_D(\vec{\boldsymbol{\tau}}_h), \tag{2.22a}$$

$$\mathbf{a}(\varphi_h, \psi_h) + \mathbf{b}(\psi_h, \lambda_{\widetilde{h}}) = F_{\mathbf{u}_h,\varphi_h}(\psi_h), \tag{2.22b}$$

$$\mathbf{b}(\varphi_h, \xi_{\widetilde{h}}) = G(\xi_{\widetilde{h}}), \tag{2.22c}$$

for all $(\vec{\boldsymbol{\tau}}_h, (\psi_h, \xi_{\widetilde{h}})) \in \mathbb{H}^{\boldsymbol{\sigma}}_h \times \mathbf{H}^{\mathbf{u}}_h \times \mathbb{H}^{\gamma}_h \times \mathrm{H}^{\varphi}_h \times \mathrm{H}^{\lambda}_{\widetilde{h}}$, where the forms $\mathbf{A}_{\varphi_h}$, $\mathbf{B}_{\mathbf{u}_h,\varphi_h}$, $\mathbf{a}$, and $\mathbf{b}$; and the functionals F_{φ_h}, F_D, $F_{\mathbf{u}_h,\varphi_h}$ and G are defined by (2.7)-(2.14). A similar analysis to the one realized for the proof of well-posedness of (2.6) leads to the existence of $(\vec{\boldsymbol{\sigma}}_h, (\varphi_h, \lambda_{\widetilde{h}})) \in \mathbb{H}^{\boldsymbol{\sigma}}_h \times \mathbf{H}^{\mathbf{u}}_h \times \mathbb{H}^{\gamma}_h \times \mathrm{H}^{\varphi}_h \times \mathrm{H}^{\lambda}_{\widetilde{h}}$ solution to (2.22), with $(\mathbf{u}_h, \varphi_h) \in W_h := \{(\mathbf{w}_h, \phi_h) \in \mathbf{H}^{\mathbf{u}}_h \times \mathrm{H}^{\varphi}_h : \|(\mathbf{w}, \phi)\| \leq r\}$ and $r \in (0, r_0)$ (cf. [1, Theorem 4.8]). Moreover, there hold

$$\|\vec{\boldsymbol{\sigma}}_h\| \leq C_{\mathbf{S}} \left\{ r \|\mathbf{g}\|_{\infty,\Omega} + \|\mathbf{u}_D\|_{1/2,\Gamma} + \|\mathbf{u}_D\|_{0,\Gamma} \right\} \tag{2.23}$$

and

$$\left\| (\varphi_h, \lambda_{\widetilde{h}}) \right\| \leq \widetilde{C}_{\widetilde{\mathbf{S}}} \left\{ r \|\mathbf{u}_h\|_{1,\Omega} + \|\varphi_D\|_{1/2,\Gamma} \right\}. \tag{2.24}$$

with $C_{\mathbf{S}}$, $\widetilde{C}_{\widetilde{\mathbf{S}}}$ being positive constants independent of h and $\widetilde{h}$. We also mention that when using these finite element spaces, optimal rates of convergence are achieved for all the discrete variables, including the postprocessed pressure (cf. [1, Theorem 5.6] and the numerical examples therein).

3 A posteriori error analysis

This section constitutes the main contribution of the present work. Here, we develop a reliable and efficient residual-based a posteriori error estimator for (2.6) and (2.22).

3.1 Preliminaries

We introduce next some notations that will be used throughout this section to describe local information on elements and edges. First, let $\mathcal{E}_h$ be the set of edges $e \in \mathcal{T}_h$, whose corresponding diameters are denoted by h_e, and define

$$\mathcal{E}_h(\Omega) := \{e \in \mathcal{E}_h : e \subseteq \Omega\}, \quad \mathcal{E}_h(\Gamma) := \{e \in \mathcal{E}_h : e \subseteq \Gamma\},$$

and

$$\mathcal{E}_h(T) := \{e \in \mathcal{E}_h : e \subseteq \partial T\} \quad \forall\, T \in \mathcal{T}_h.$$

Thus, the usual jump operator $[\![\cdot]\!]$ across an internal edge $e \in \mathcal{E}_h(\Omega)$ is defined for piecewise continuous matrix, vector, or scalar-valued functions $\boldsymbol{\zeta}$ as

$$[\![\boldsymbol{\zeta}]\!] = \boldsymbol{\zeta}\big|_{T_+} - \boldsymbol{\zeta}\big|_{T_-},$$

where T_- and T_+ are the triangles of $\mathcal{T}_h$ sharing the edge e. In addition, if $\boldsymbol{\psi} = (\psi_1, \psi_2)$ and $\boldsymbol{\zeta} = (\zeta_{ij})_{1\le i,j\le 2}$ are vector-valued and matrix-valued functions, respectively, we set the differential operators

$$\underline{\mathbf{curl}}\,(\boldsymbol{\psi}) := \begin{pmatrix} \dfrac{\partial \psi_1}{\partial x_2} & -\dfrac{\partial \psi_1}{\partial x_1} \\ \dfrac{\partial \psi_2}{\partial x_2} & -\dfrac{\partial \psi_2}{\partial x_1} \end{pmatrix}, \quad \mathrm{curl}\,(\boldsymbol{\zeta}) := \begin{pmatrix} \dfrac{\partial \zeta_{12}}{\partial x_1} - \dfrac{\partial \zeta_{11}}{\partial x_2} \\ \dfrac{\partial \psi_{22}}{\partial x_1} - \dfrac{\partial \zeta_{21}}{\partial x_2} \end{pmatrix}.$$

We also define the unit tangential vector $\boldsymbol{s}$ on each edge $e \in \mathcal{E}_h$ by $\boldsymbol{s} := (-\nu_2, \nu_1)^{\mathtt{t}}$ where $\boldsymbol{\nu} = (\nu_1, \nu_2)^{\mathtt{t}}$ is the usual unit normal vector. That being said, let us introduce the global a posteriori error estimator

$$\boldsymbol{\theta} := \left\{ \sum_{T\in\mathcal{T}_h} \boldsymbol{\theta}_T^2 + \|\, \varphi_D - \varphi_h \,\|_{1/2,\Gamma}^2 \right\}^{1/2}, \tag{3.1}$$

where $\boldsymbol{\theta}_T$ is the local indicator defined for each $T \in \mathcal{T}_h$ by

$$\begin{aligned} \boldsymbol{\theta}_T^2 :=\; & \|\, \mathbf{e}(\mathbf{u}_h) - \mu(\varphi_h)^{-1}(\mathbf{u}_h\otimes\mathbf{u}_h + \boldsymbol{\sigma}_h)^{\mathtt{d}} \,\|_{0,T}^2 + \|\, \boldsymbol{\sigma}_h - \boldsymbol{\sigma}_h^{\mathtt{t}} \,\|_{0,T}^2 + \|\, \boldsymbol{\gamma}_h - \boldsymbol{\omega}(\mathbf{u}_h) \,\|_{0,T}^2 \\ & + \|\, \mathbf{div}\,\boldsymbol{\sigma}_h + \varphi_h \mathbf{g} \,\|_{0,T}^2 + h_T^2 \left\| \, \mathrm{curl}\left\{ \boldsymbol{\gamma}_h + \mu(\varphi_h)^{-1}(\mathbf{u}_h\otimes\mathbf{u}_h + \boldsymbol{\sigma}_h)^{\mathtt{d}} \right\} \right\|_{0,T}^2 \\ & + h_T^2 \,\|\, \mathrm{div}\,(\mathbb{K}\nabla\varphi_h) - \mathbf{u}_h\cdot\nabla\varphi_h \,\|_{0,T}^2 \\ & + \sum_{e\in\mathcal{E}_h(T)\cap\mathcal{E}_h(\Omega)} h_e \left\{ \|\, [\![\{\boldsymbol{\gamma}_h + \mu(\varphi_h)^{-1}(\mathbf{u}_h\otimes\mathbf{u}_h + \boldsymbol{\sigma}_h)^{\mathtt{d}}\}\boldsymbol{s}]\!] \,\|_{0,e}^2 + \|\, [\![\mathbb{K}\nabla\varphi_h\cdot\boldsymbol{\nu}]\!] \,\|_{0,e}^2 \right\} \\ & + \sum_{e\in\mathcal{E}_h(T)\cap\mathcal{E}_h(\Gamma)} \left\{ h_e \left\| \, \{\boldsymbol{\gamma}_h + \mu(\varphi_h)^{-1}(\mathbf{u}_h\otimes\mathbf{u}_h + \boldsymbol{\sigma}_h)^{\mathtt{d}}\}\boldsymbol{s} - \frac{\mathrm{d}\mathbf{u}_D}{\mathrm{d}\boldsymbol{s}} \right\|_{0,e}^2 \right. \\ & \left. + h_e \,\|\, \lambda_{\widetilde{h}} + \mathbb{K}\nabla\varphi_h\cdot\boldsymbol{\nu} \,\|_{0,e}^2 + \|\, \mathbf{u}_D - \mathbf{u}_h \,\|_{0,e}^2 \right\}. \end{aligned} \tag{3.2}$$

The residual character of each term defining $\boldsymbol{\theta}_T$ becomes clear by having a look at the strong problem (2.5) and to the regularity of the continuous weak solution. We remark in advance that further regularity will be assumed for $\mathbf{u}_D$, so that the previous estimator is well-defined. In addition, since $\boldsymbol{\theta}$ is not fully local due to the last term in (3.1), we will show (see Section 3.4) that this estimator induces another one that is is indeed fully computable, which will allow us to construct an adaptive refinement algorithm. We also mention that, for the upcoming analysis, the further regularity assumption made for the mixed formulation of the momentum equation will be considered here as well. Indeed, we assume that for some $\varepsilon \in (0,1)$, $\mathbf{u}_D \in \mathbf{H}^{1/2+\varepsilon}(\Gamma)$, and that for each $(\mathbf{w},\phi) \in \mathbf{H}^1(\Omega)\times \mathrm{H}^1(\Omega)$ with $\|\, \mathbf{w} \,\|_{1,\Omega} \le r$, $r > 0$ given, the unique solution to the mixed formulation of the momentum equation, that is: Find $\vec{\boldsymbol{\zeta}} := (\boldsymbol{\zeta}, \mathbf{z}, \boldsymbol{\chi}) \in \mathbb{H}_0(\mathbf{div};\Omega)\times\mathbf{H}^1(\Omega)\times\mathbb{L}^2_{\mathtt{skew}}(\Omega)$ such that

$$\mathbf{A}_\phi(\vec{\boldsymbol{\zeta}}, \vec{\boldsymbol{\tau}}) + \mathbf{B}_{\mathbf{w},\phi}(\vec{\boldsymbol{\zeta}}, \vec{\boldsymbol{\tau}}) = F_D(\vec{\boldsymbol{\tau}}) + F_\phi(\vec{\boldsymbol{\tau}}) \quad \forall\, \vec{\boldsymbol{\tau}} \in \mathbb{H}_0(\mathbf{div};\Omega)\times\mathbf{H}^1(\Omega)\times\mathbb{L}^2_{\mathtt{skew}}(\Omega),$$

also satisfies $\vec{\boldsymbol{\zeta}} \in \mathbb{H}_0(\mathbf{div};\Omega)\cap\mathbb{H}^\varepsilon(\Omega)\times\mathbf{H}^{1+\varepsilon}(\Omega)\times\mathbb{L}^2_{\mathtt{skew}}(\Omega)\cap\mathbb{H}^\varepsilon(\Omega)$ and

$$\|\, \boldsymbol{\zeta} \,\|_{\varepsilon,\Omega} + \|\, \mathbf{z} \,\|_{1+\varepsilon,\Omega} + \|\, \boldsymbol{\chi} \,\|_{\varepsilon,\Omega} \le \widetilde{C}_{\mathbf{S}}(r) \Big\{ \|\, \mathbf{g} \,\|_{\infty,\Omega} \|\, \phi \,\|_{1,\Omega} + \|\, \mathbf{u}_D \,\|_{1/2+\varepsilon,\Gamma} + \|\, \mathbf{u}_D \,\|_{0,\Gamma} \Big\}, \tag{3.3}$$

with $\widetilde{C}_{\mathbf{S}}(r)$ being a positive constant independent of $\mathbf{w}$ but depending on the upper bound r of its $\mathbf{H}^1$-norm.

3.2 Reliability

The main result of this section reads as follows.

Theorem 3.1. *Let* $(\vec{\boldsymbol{\sigma}}, (\varphi, \lambda))$ *and* $(\vec{\boldsymbol{\sigma}}_h, (\varphi_h, \lambda_{\widetilde{h}}))$ *be solutions to* (2.6) *and* (2.22)*, respectively. Then* $\boldsymbol{\theta}$ *is a reliable estimator, i.e., there exists a positive constant* $C_{\rm rel}$*, depending on physical and stabilization parameters, but independent of* h *and* $\widetilde{h}$*, such that*

$$\left\| (\vec{\boldsymbol{\sigma}}, (\varphi, \lambda)) - (\vec{\boldsymbol{\sigma}}_h, (\varphi_h, \lambda_{\widetilde{h}})) \right\| \le C_{\rm rel}\, \boldsymbol{\theta},$$

provided $\mathbf{u}_D \in \mathbf{H}^1(\Gamma)$ *and the data are small enough (cf. Lemma* 3.4*).*

The proof of the foregoing theorem is separated into the following two subsections.

3.2.1 A first error estimate

Lemma 3.2. *There exists* $\bar{C}_1 > 0$*, independent of* h*, such that*

$$\begin{aligned}\| \vec{\boldsymbol{\sigma}} - \vec{\boldsymbol{\sigma}}_h \| \le \bar{C}_1 \Big\{ & \left\| \mathbf{e}(\mathbf{u}_h) - \mu(\varphi_h)^{-1}(\mathbf{u}_h \otimes \mathbf{u}_h + \boldsymbol{\sigma}_h)^{\mathtt{d}} \right\|_{0,\Omega} + \| \mathbf{div}\, \boldsymbol{\sigma}_h + \varphi_h \mathbf{g} \|_{0,\Omega} \\ & + \| \mathbf{u}_D - \mathbf{u}_h \|_{0,\Gamma} + \left\| \boldsymbol{\sigma}_h - \boldsymbol{\sigma}_h^{\mathtt{t}} \right\|_{0,\Omega} + \| \boldsymbol{\gamma}_h - \boldsymbol{\omega}(\mathbf{u}_h) \|_{0,\Omega} + \frac{\mu_2}{\mu_1^2} \| \boldsymbol{\sigma} - \boldsymbol{\sigma}_h \|_{\mathrm{div};\Omega} \\ & + \| \mathbf{u}_h \|_{1,\Omega} \| \mathbf{u} - \mathbf{u}_h \|_{1,\Omega} + \Big(\| \mathbf{g} \|_{\infty,\Omega} + \| \boldsymbol{\sigma} \|_{\varepsilon,\Omega} + \| \mathbf{u}_h \|_{1,\Omega}^2 \Big) \| \varphi - \varphi_h \|_{1,\Omega} + \| \mathcal{R}^{\mathtt{m}} \| \Big\},\end{aligned} \tag{3.4}$$

where $\mathcal{R}^{\mathtt{m}} : \mathbb{H}_0(\mathbf{div}; \Omega) \to R$ *is the linear and bounded functional defined as*

$$\mathcal{R}^{\mathtt{m}}(\boldsymbol{\tau}) := F_{\varphi_h}(\boldsymbol{\tau}, \mathbf{0}, \mathbf{0}) + F_D(\boldsymbol{\tau}, \mathbf{0}, \mathbf{0}) - \mathbf{A}_{\varphi_h}(\vec{\boldsymbol{\sigma}}_h, (\boldsymbol{\tau}, \mathbf{0}, \mathbf{0})) - \mathbf{B}_{\mathbf{u}_h,\varphi_h}(\vec{\boldsymbol{\sigma}}_h, (\boldsymbol{\tau}, \mathbf{0}, \mathbf{0})), \tag{3.5}$$

that is,

$$\begin{aligned}\mathcal{R}^{\mathtt{m}}(\boldsymbol{\tau}) = -\kappa_2 \int_\Omega \varphi_h \mathbf{g} \cdot \mathbf{div}\, \boldsymbol{\tau} + \langle \boldsymbol{\tau}\boldsymbol{\nu}, \mathbf{u}_D \rangle_\Gamma - \int_\Omega \frac{1}{\mu(\varphi_h)} \boldsymbol{\sigma}_h^{\mathtt{d}} : \boldsymbol{\tau} - \int_\Omega \mathbf{u}_h \cdot \mathbf{div}\, \boldsymbol{\tau} \\ - \kappa_2 \int_\Omega \mathbf{div}\, \boldsymbol{\sigma}_h \cdot \boldsymbol{\tau} - \int_\Omega \boldsymbol{\gamma}_h : \boldsymbol{\tau} - \int_\Omega \frac{1}{\mu(\varphi_h)} (\mathbf{u}_h \otimes \mathbf{u}_h)^{\mathtt{d}} : \boldsymbol{\tau},\end{aligned} \tag{3.6}$$

for all $\boldsymbol{\tau} \in \mathbb{H}_0(\mathbf{div}; \Omega)$.

Proof. Since $(\mathbf{u}, \varphi) \in W$, [1, Eq. (3.37)] shows that the bilinear form $\mathbf{A}_\varphi + \mathbf{B}_{\mathbf{u},\varphi}$ is uniformly elliptic in $\mathbb{H}_0(\mathbf{div}; \Omega) \times \mathbf{H}^1(\Omega) \times \mathbb{L}^2_{\mathtt{skew}}(\Omega)$ with a constant $\widehat{\alpha}(\Omega) > 0$ depending on Ω, and hence the following inf-sup condition holds

$$\sup_{\substack{\vec{\boldsymbol{\tau}} \in \mathbb{H}_0(\mathbf{div};\Omega) \times \mathbf{H}^1(\Omega) \times \mathbb{L}^2_{\mathtt{skew}}(\Omega) \\ \vec{\boldsymbol{\tau}} \neq \vec{\mathbf{0}}}} \frac{(\mathbf{A}_\varphi + \mathbf{B}_{\mathbf{u},\varphi})(\vec{\boldsymbol{\zeta}}, \vec{\boldsymbol{\tau}})}{\| \vec{\boldsymbol{\tau}} \|} \ge \widehat{\alpha}(\Omega) \left\| \vec{\boldsymbol{\zeta}} \right\| \tag{3.7}$$

for all $\vec{\boldsymbol{\zeta}} \in \mathbb{H}_0(\mathbf{div}; \Omega) \times \mathbf{H}^1(\Omega) \times \mathbb{L}^2_{\mathtt{skew}}(\Omega)$. In particular, taking $\vec{\boldsymbol{\zeta}} = \vec{\boldsymbol{\sigma}} - \vec{\boldsymbol{\sigma}}_h$, from (2.6a) we can write for any $\vec{\boldsymbol{\tau}} \in \mathbb{H}_0(\mathbf{div}; \Omega) \times \mathbf{H}^1(\Omega) \times \mathbb{L}^2_{\mathtt{skew}}(\Omega)$

$$\begin{aligned}(\mathbf{A}_\varphi + \mathbf{B}_{\mathbf{u},\varphi})(\vec{\boldsymbol{\sigma}} - \vec{\boldsymbol{\sigma}}_h, \vec{\boldsymbol{\tau}}) = F_{\varphi - \varphi_h}(\vec{\boldsymbol{\tau}}) + (\mathbf{A}_{\varphi_h} - \mathbf{A}_\varphi)(\vec{\boldsymbol{\sigma}}_h, \vec{\boldsymbol{\tau}}) + (\mathbf{B}_{\mathbf{u}_h,\varphi_h} - \mathbf{B}_{\mathbf{u}_h,\varphi})(\vec{\boldsymbol{\sigma}}_h, \vec{\boldsymbol{\tau}}) \\ + (\mathbf{B}_{\mathbf{u}_h,\varphi} - \mathbf{B}_{\mathbf{u},\varphi})(\vec{\boldsymbol{\sigma}}_h, \vec{\boldsymbol{\tau}}) + F_D(\vec{\boldsymbol{\tau}}) + F_{\varphi_h}(\vec{\boldsymbol{\tau}}) - \mathbf{A}_{\varphi_h}(\vec{\boldsymbol{\sigma}}_h, \vec{\boldsymbol{\tau}}) - \mathbf{B}_{\mathbf{u}_h,\varphi_h}(\vec{\boldsymbol{\sigma}}_h, \vec{\boldsymbol{\tau}}),\end{aligned}$$

which back into (3.7) results in

$$\widehat{\alpha}(\Omega) \| \vec{\boldsymbol{\sigma}} - \vec{\boldsymbol{\sigma}}_h \| \le \sup_{\substack{\vec{\boldsymbol{\tau}} \in \mathbb{H}_0(\mathbf{div};\Omega) \times \mathbf{H}^1(\Omega) \times \mathbb{L}^2_{\mathtt{skew}}(\Omega) \\ \vec{\boldsymbol{\tau}} \neq \vec{\mathbf{0}}}} \frac{\mathcal{S}(\vec{\boldsymbol{\tau}}) + \mathcal{P}(\mathbf{v}) + \mathcal{Q}(\boldsymbol{\eta}) + \mathcal{R}^{\mathtt{m}}(\boldsymbol{\tau})}{\| \vec{\boldsymbol{\tau}} \|}, \tag{3.8}$$

where the functionals $\mathcal{S} \in [\mathbb{H}_0(\mathbf{div};\Omega) \times \mathbf{H}^1(\Omega) \times \mathbb{L}^2_{\mathtt{skew}}(\Omega)]'$, $\mathcal{P} \in \mathbf{H}^1(\Omega)'$, $\mathcal{Q} \in \mathbb{L}^2_{\mathtt{skew}}(\Omega)'$ are given by

$$\mathcal{S}(\vec{\boldsymbol{\tau}}) := F_{\varphi-\varphi_h}(\vec{\boldsymbol{\tau}}) + (\mathbf{A}_{\varphi_h} - \mathbf{A}_{\varphi})(\vec{\boldsymbol{\sigma}}_h, \vec{\boldsymbol{\tau}}) + (\mathbf{B}_{\mathbf{u}_h,\varphi_h} - \mathbf{B}_{\mathbf{u}_h,\varphi})(\vec{\boldsymbol{\sigma}}_h, \vec{\boldsymbol{\tau}}) + (\mathbf{B}_{\mathbf{u}_h,\varphi} - \mathbf{B}_{\mathbf{u},\varphi})(\vec{\boldsymbol{\sigma}}_h, \vec{\boldsymbol{\tau}})$$

$$\mathcal{P}(\mathbf{v}) := F_{\varphi_h}(\mathbf{0},\mathbf{v},\mathbf{0}) + F_D(\mathbf{0},\mathbf{v},\mathbf{0}) - \mathbf{A}_{\varphi_h}(\vec{\boldsymbol{\sigma}}_h, (\mathbf{0},\mathbf{v},\mathbf{0})) - \mathbf{B}_{\mathbf{u}_h,\varphi_h}(\vec{\boldsymbol{\sigma}}_h, (\mathbf{0},\mathbf{v},\mathbf{0})),$$

$$\mathcal{Q}(\boldsymbol{\eta}) := F_{\varphi_h}(\mathbf{0},\mathbf{0},\boldsymbol{\eta}) + F_D(\mathbf{0},\mathbf{0},\boldsymbol{\eta}) - \mathbf{A}_{\varphi_h}(\vec{\boldsymbol{\sigma}}_h, (\mathbf{0},\mathbf{0},\boldsymbol{\eta})) - \mathbf{B}_{\mathbf{u}_h,\varphi_h}(\vec{\boldsymbol{\sigma}}_h, (\mathbf{0},\mathbf{0},\boldsymbol{\eta}))\,,$$

that is,

$$\begin{aligned} \mathcal{S}(\vec{\boldsymbol{\tau}}) = & \int_\Omega (\varphi - \varphi_h)\mathbf{g} \cdot \Big\{ \mathbf{v} - \kappa_2 \mathbf{div}\,\boldsymbol{\tau} \Big\} + \int_\Omega \frac{\mu(\varphi_h) - \mu(\varphi)}{\mu(\varphi)\mu(\varphi_h)} \boldsymbol{\sigma}_h^{\mathtt{d}} : \Big\{ \boldsymbol{\tau}^{\mathtt{d}} - \kappa_1 \mathbf{e}(\mathbf{v}) \Big\} \\ & + \int_\Omega \frac{1}{\mu(\varphi)} [\mathbf{u}_h \otimes (\mathbf{u}_h - \mathbf{u})]^{\mathtt{d}} : \Big\{ \boldsymbol{\tau}^{\mathtt{d}} - \kappa_1 \mathbf{e}(\mathbf{v}) \Big\} \\ & + \int_\Omega \frac{\mu(\varphi) - \mu(\varphi_h)}{\mu(\varphi)\mu(\varphi_h)} (\mathbf{u}_h \otimes \mathbf{u}_h)^{\mathtt{d}} : \Big\{ \boldsymbol{\tau}^{\mathtt{d}} - \kappa_1 \mathbf{e}(\mathbf{v}) \Big\}, \end{aligned} \tag{3.9}$$

$$\begin{aligned} \mathcal{P}(\mathbf{v}) = & \int_\Omega \varphi_h \mathbf{g} \cdot \mathbf{v} + \kappa_4 \int_\Gamma \mathbf{u}_D \cdot \mathbf{v} + \kappa_1 \int_\Omega \frac{1}{\mu(\varphi_h)} \boldsymbol{\sigma}_h^{\mathtt{d}} : \mathbf{e}(\mathbf{v}) - \kappa_1 \int_\Omega \mathbf{e}(\mathbf{u}_h) : \mathbf{e}(\mathbf{v}) \\ & + \int_\Omega \mathbf{v} \cdot \mathbf{div}\,\boldsymbol{\sigma}_h - \kappa_4 \int_\Gamma \mathbf{u}_h \cdot \mathbf{v} + \kappa_1 \int_\Omega \frac{1}{\mu(\varphi_h)} (\mathbf{u}_h \otimes \mathbf{u}_h)^{\mathtt{d}} : \mathbf{e}(\mathbf{v}), \end{aligned} \tag{3.10}$$

$$\mathcal{Q}(\boldsymbol{\eta}) = \int_\Omega \boldsymbol{\sigma}_h : \boldsymbol{\eta} - \kappa_3 \int_\Omega \Big\{ \boldsymbol{\gamma}_h - \boldsymbol{\omega}(\mathbf{u}_h) \Big\} : \boldsymbol{\eta}, \tag{3.11}$$

and $\mathcal{R}^{\mathtt{m}}$ is defined as in (3.6). We show next that $\mathcal{S}$, $\mathcal{P}$ and $\mathcal{Q}$ are indeed bounded (their linear character is clear). For $\mathcal{P}$, a simple application of the Cauchy-Schwarz inequality and the trace theorem with constant $c_0(\Omega)$ leads us to

$$\begin{aligned} |\mathcal{P}(\mathbf{v})| \le \max\{\kappa_1, 1, \kappa_4 c_0(\Omega)\} \Big\{ & \| \mathbf{e}(\mathbf{u}_h) - \mu(\varphi_h)^{-1} (\mathbf{u}_h \otimes \mathbf{u}_h + \boldsymbol{\sigma}_h)^{\mathtt{d}} \|_{0,\Omega} \\ & + \| \mathbf{div}\,\boldsymbol{\sigma}_h + \varphi_h \mathbf{g} \|_{0,\Omega} + \| \mathbf{u}_D - \mathbf{u}_h \|_{0,\Gamma} \Big\} \| \mathbf{v} \|_{1,\Omega} \quad \forall\, \mathbf{v} \in \mathbf{H}^1(\Omega), \end{aligned} \tag{3.12}$$

whereas for $\mathcal{Q}$, we follow the ideas in [14] and decompose the discrete pseudostress tensor into its symmetric and skew-symmetric part to construct a residual expression for this functional. Thus,

$$\mathcal{Q}(\boldsymbol{\eta}) = \frac{1}{2} \int_\Omega \Big\{ \boldsymbol{\sigma}_h - \boldsymbol{\sigma}_h^{\mathtt{t}} \Big\} : \boldsymbol{\eta} - \kappa_3 \int_\Omega [\boldsymbol{\gamma}_h - \boldsymbol{\omega}(\mathbf{u}_h)] : \boldsymbol{\eta} \quad \forall\, \boldsymbol{\eta} \in \mathbb{L}^2_{\mathtt{skew}}(\Omega),$$

which yields

$$|\mathcal{Q}(\boldsymbol{\eta})| \le \max\left\{ \frac{1}{2}, \kappa_3 \right\} \Big\{ \| \boldsymbol{\sigma}_h - \boldsymbol{\sigma}_h^{\mathtt{t}} \|_{0,\Omega} + \| \boldsymbol{\gamma}_h - \boldsymbol{\omega}(\mathbf{u}_h) \|_{0,\Omega} \Big\} \| \boldsymbol{\eta} \|_{0,\Omega} \quad \forall\, \boldsymbol{\eta} \in \mathbb{L}^2_{\mathtt{skew}}(\Omega). \tag{3.13}$$

Finally, for $\mathcal{S}$, we add and subtract $\boldsymbol{\sigma}^{\mathtt{d}}$ in the second term of the right-hand side of (3.9), and then we use the Hölder inequality and several continuous injections as in [1, Lemma 3.8] to obtain

$$\begin{aligned} |\mathcal{S}(\vec{\boldsymbol{\tau}})| \le \Big\{ & (2+\kappa_2^2)^{1/2} \| \mathbf{g} \|_{\infty,\Omega} \| \varphi - \varphi_h \|_{1,\Omega} + \frac{2\mu_2 (2+\kappa_1^2)^{1/2}}{\mu_1^2} \| \boldsymbol{\sigma} - \boldsymbol{\sigma}_h \|_{0,\Omega} \\ & + \frac{L_\mu (2+\kappa_1^2)^{1/2} C_\varepsilon \widetilde{C}_\varepsilon}{\mu_1^2} \| \varphi - \varphi_h \|_{1,\Omega} \| \boldsymbol{\sigma} \|_{\varepsilon,\Omega} + \frac{c_1(\Omega)(2+\kappa_1^2)^{1/2}}{\mu_1} \| \mathbf{u}_h \|_{1,\Omega} \| \mathbf{u} - \mathbf{u}_h \|_{1,\Omega} \\ & + \frac{c_1(\Omega)(2+\kappa_1^2)^{1/2} C_i}{\mu_1} \| \varphi - \varphi_h \|_{1,\Omega} \| \mathbf{u}_h \|_{1,\Omega}^2 \Big\} \| \vec{\boldsymbol{\tau}} \|, \end{aligned} \tag{3.14}$$

where $c_1(\Omega) > 0$ is a constant arising from the inequality [1, Eq. 3.6] and the boundedness constant C_ε corresponds to $\mathrm{H}^\varepsilon(\Omega) \hookrightarrow \mathrm{L}^{2/(1-\varepsilon)}(\Omega)$, $\widetilde{C}_\varepsilon$ to $\mathrm{H}^1(\Omega) \hookrightarrow \mathrm{L}^{2/\varepsilon}(\Omega)$, and C_i to the injections $\mathrm{H}^1(\Omega) \hookrightarrow \mathrm{L}^4(\Omega)$ and $\mathrm{H}^1(\Omega) \hookrightarrow \mathrm{L}^8(\Omega)$. Hence, there exists $c_1, c_2, c_3 > 0$ such that

$$|\mathcal{S}(\vec{\boldsymbol{\tau}})| \le \Big\{ c_1 \Big(\| \mathbf{g} \|_{\infty,\Omega} + \| \boldsymbol{\sigma} \|_{\varepsilon,\Omega} + \| \mathbf{u}_h \|_{1,\Omega}^2 \Big) \| \varphi - \varphi_h \|_{1,\Omega} + c_2 \frac{\mu_2}{\mu_1^2} \| \boldsymbol{\sigma} - \boldsymbol{\sigma}_h \|_{\mathbf{div};\Omega} + c_3 \| \mathbf{u}_h \|_{1,\Omega} \| \mathbf{u} - \mathbf{u}_h \|_{1,\Omega} \Big\} \| \vec{\boldsymbol{\tau}} \|, \tag{3.15}$$

for all $\vec{\boldsymbol{\tau}} \in \mathbb{H}_0(\mathbf{div};\Omega) \times \mathbf{H}^1(\Omega) \times \mathbb{L}^2_{\mathtt{skew}}(\Omega)$. Therefore, putting (3.15), together with (3.12) and (3.13), back into (3.8), we get (3.4), concluding this way the proof. □

Regarding a preliminary bound for $\| (\varphi, \lambda) - (\varphi_h, \lambda_{\widetilde{h}}) \|$, we cite the following result from [9], which uses a similar technique to the foregoing Lemma, but now beginning from a global inf-sup condition that comes as a consequence of the well-posedness of the primal formulation of the energy equation.

Lemma 3.3. *There exists a positive constant $\bar{C}_2 > 0$ independent of h and $\widetilde{h}$ such that*

$$\| (\varphi, \lambda) - (\varphi_h, \lambda_{\widetilde{h}}) \| \le \bar{C}_2 \Big\{ \| \varphi \|_{1,\Omega} \| \mathbf{u} - \mathbf{u}_h \|_{1,\Omega} + \| \mathbf{u}_h \|_{1,\Omega} \| \varphi - \varphi_h \|_{1,\Omega} + \| \varphi_D - \varphi_h \|_{1/2,\Gamma} + \| \mathcal{R}^{\mathtt{e}} \| \Big\}, \tag{3.16}$$

where $\mathcal{R}^{\mathtt{e}} : \mathrm{H}^1(\Omega) \to \mathrm{R}$ is the linear and bounded functional defined as

$$\mathcal{R}^{\mathtt{e}}(\psi) := F_{\mathbf{u}_h,\varphi_h}(\psi) - \mathbf{a}(\varphi_h, \psi) - \mathbf{b}(\psi, \lambda_{\widetilde{h}}),$$

that is,

$$\mathcal{R}^{\mathtt{e}}(\psi) = - \int_\Omega \psi \mathbf{u}_h \cdot \nabla \varphi_h - \int_\Omega \mathbb{K} \nabla \varphi_h \cdot \nabla \psi - \langle \lambda_{\widetilde{h}}, \psi \rangle_\Gamma, \tag{3.17}$$

for all $\psi \in \mathrm{H}^1(\Omega)$.

Proof. See [9, Lemma 3.3]. □

With the results from the previous two lemmas, we can now construct a first estimate for the total error. Indeed, from (3.4) and (3.16) we have

$$\begin{aligned} \| (\vec{\boldsymbol{\sigma}}, (\varphi, \lambda)) - (\vec{\boldsymbol{\sigma}}_h, (\varphi_h, \lambda_{\widetilde{h}})) \| &\le \bar{C}_1 \| \mathbf{e}(\mathbf{u}_h) - \mu(\varphi_h)^{-1} (\mathbf{u}_h \otimes \mathbf{u}_h + \boldsymbol{\sigma}_h)^{\mathtt{d}} \|_{0,\Omega} \\ &+ \bar{C}_1 \| \mathbf{div}\, \boldsymbol{\sigma}_h + \varphi_h \mathbf{g} \|_{0,\Omega} + \bar{C}_1 \| \mathbf{u}_D - \mathbf{u}_h \|_{0,\Gamma} + \bar{C}_1 \| \boldsymbol{\sigma}_h - \boldsymbol{\sigma}_h^{\mathtt{t}} \|_{0,\Omega} \\ &+ \bar{C}_1 \| \boldsymbol{\gamma}_h - \boldsymbol{\omega}(\mathbf{u}_h) \|_{0,\Omega} + \Big\{ \bar{C}_1 \frac{\mu_2}{\mu_1^2} + \bar{C}_1 \| \mathbf{g} \|_{\infty,\Omega} + \bar{C}_1 \| \boldsymbol{\sigma} \|_{\varepsilon,\Omega} \\ &+ (\bar{C}_1 + \bar{C}_2) \| \mathbf{u}_h \|_{1,\Omega} + \bar{C}_1 \| \mathbf{u}_h \|_{1,\Omega}^2 + \bar{C}_2 \| \varphi \|_{1,\Omega} \Big\} \| (\vec{\boldsymbol{\sigma}}, (\varphi, \lambda)) - (\vec{\boldsymbol{\sigma}}_h, (\varphi_h, \lambda_{\widetilde{h}})) \| \\ &+ \bar{C}_1 \| \mathcal{R}^{\mathtt{m}} \| + \bar{C}_2 \| \mathcal{R}^{\mathtt{e}} \| + \bar{C}_2 \| \varphi_D - \varphi_h \|_{1/2,\Gamma}. \end{aligned}$$

Then, we use the continuous dependence results (2.15), (2.16) and (2.23) to bound the terms $\| \varphi \|_{1,\Omega}$ and $\| \mathbf{u}_h \|_{1,\Omega}$, and the further regularity assumed for $\boldsymbol{\sigma}$ in (3.3) to bound $\| \boldsymbol{\sigma} \|_{\varepsilon,\Omega}$ by data. In this way, defining

$$\mathbf{C}_0(\mathbf{g}, \mathbf{u}_D) := C_{\mathbf{S}} \left\{ r \| \mathbf{g} \|_{\infty,\Omega} + \| \mathbf{u}_D \|_{1/2,\Gamma} + \| \mathbf{u}_D \|_{0,\Gamma} \right\},$$

$$\mathbf{C}_{0,\varepsilon}(\mathbf{g}, \mathbf{u}_D) := \widetilde{C}_{\mathbf{S}}(r) \left\{ r \| \mathbf{g} \|_{\infty,\Omega} + \| \mathbf{u}_D \|_{1/2+\varepsilon,\Gamma} + \| \mathbf{u}_D \|_{0,\Gamma} \right\},$$

and

$$\bar{\mathbf{C}}(\mathbf{g},\mathbf{u}_D,\varphi_D) := \bar{C}_1\|\,\mathbf{g}\,\|_{\infty,\Omega} + \bar{C}_1\mathbf{C}_{0,\varepsilon}(\mathbf{g},\mathbf{u}_D) + \bar{C}_1\mathbf{C}_0(\mathbf{g},\mathbf{u}_D)^2 \\ + (\bar{C}_1 + \bar{C}_2 + \bar{C}_2 C_{\widetilde{\mathbf{S}}} r)\mathbf{C}_0(\mathbf{g},\mathbf{u}_D) + \bar{C}_2 C_{\widetilde{\mathbf{S}}}\|\,\varphi_D\,\|_{1/2,\Gamma},$$

we get the following result.

Lemma 3.4. *Assume that*

$$\bar{C}_1\frac{\mu_2}{\mu_1^2} < \frac{1}{2} \quad \textit{and} \quad \bar{\mathbf{C}}(\mathbf{g},\mathbf{u}_D,\varphi_D) < \frac{1}{2}.$$

Then, there exists a constant $\bar{C} > 0$ such that the total error satisfies

$$\|\,(\vec{\boldsymbol{\sigma}},(\varphi,\lambda)) - (\vec{\boldsymbol{\sigma}}_h,(\varphi_h,\lambda_{\widetilde{h}}))\,\| \le \bar{C}\Big\{\|\,\mathbf{e}(\mathbf{u}_h) - \mu(\varphi_h)^{-1}(\mathbf{u}_h\otimes\mathbf{u}_h + \boldsymbol{\sigma}_h)^{\mathtt{d}}\,\|_{0,\Omega} \\ + \|\,\mathbf{div}\,\boldsymbol{\sigma}_h + \varphi_h\mathbf{g}\,\|_{0,\Omega} + \|\,\mathbf{u}_D - \mathbf{u}_h\,\|_{0,\Gamma} + \left\|\,\boldsymbol{\sigma}_h - \boldsymbol{\sigma}_h^{\mathtt{t}}\,\right\|_{0,\Omega} \\ + \|\,\boldsymbol{\gamma}_h - \boldsymbol{\omega}(\mathbf{u}_h)\,\|_{0,\Omega} + \|\,\mathcal{R}^{\mathtt{m}}\,\| + \|\,\mathcal{R}^{\mathtt{e}}\,\| + \|\,\varphi_D - \varphi_h\,\|_{1/2,\Gamma}\Big\}.$$

Therefore, to complete the derivation of our residual-based estimator, we need to bound the norm of the residual functionals related to the momentum and energy equations, i.e., $\mathcal{R}^{\mathtt{m}}$ and $\mathcal{R}^{\mathtt{e}}$, respectively. Notice from the Galerkin scheme (2.22) that

$$\mathcal{R}^{\mathtt{m}}(\boldsymbol{\tau}_h) = 0 \quad \forall\, \boldsymbol{\tau}_h \in \mathbb{H}_h^{\boldsymbol{\sigma}}, \qquad \text{and} \qquad \mathcal{R}^{\mathtt{e}}(\psi_h) = 0 \quad \forall\, \psi_h \in \mathrm{H}_h^{\varphi},$$

whence the norms of $\mathcal{R}^{\mathtt{m}}$ and $\mathcal{R}^{\mathtt{e}}$ can be calculated as

$$\|\,\mathcal{R}^{\mathtt{m}}\,\| := \sup_{\substack{\boldsymbol{\tau}\in\mathbb{H}_0(\mathbf{div};\Omega)\\ \boldsymbol{\tau}\neq\mathbf{0}}} \frac{\mathcal{R}^{\mathtt{m}}(\boldsymbol{\tau}-\boldsymbol{\tau}_h)}{\|\,\boldsymbol{\tau}\,\|_{\mathbf{div};\Omega}}, \qquad \text{and} \qquad \|\,\mathcal{R}^{\mathtt{e}}\,\| := \sup_{\substack{\psi\in\mathrm{H}^1(\Omega)\\ \psi\neq 0}} \frac{\mathcal{R}^{\mathtt{e}}(\psi-\psi_h)}{\|\,\psi\,\|_{1,\Omega}}, \tag{3.18}$$

with $\boldsymbol{\tau}_h$ and ψ_h appropriately chosen in order to obtain local information on the error.

3.2.2 Estimating the norm of the residual functionals

We start by recalling some results associated to the main tools used throughout this section: the approximation properties of the interpolation operators of Raviart-Thomas and Clément (see, e.g., [11, 13] for their definitions) and a Helmholtz decomposition of $\mathbb{H}_0(\mathbf{div};\Omega)$.

Lemma 3.5. *Given an integer $k \ge 0$, let $\Pi_h^k : \mathbb{H}^1(\Omega) \to \mathbb{RT}_k(\mathcal{T}_h)$ be the usual Raviart-Thomas interpolation operator. Then,*

i) there exists $C > 0$ such that for each $\boldsymbol{\zeta} \in \mathbb{H}^m(\Omega)$, with $1 \le m \le k+1$, there holds

$$\left\|\,\boldsymbol{\zeta} - \Pi_h^k(\boldsymbol{\zeta})\,\right\|_{0,T} \le C h_T^m |\,\boldsymbol{\zeta}\,|_{m,T} \quad \forall\, T \in \mathcal{T}_h\,, \tag{3.19}$$

ii) there exists $C > 0$ such that for each $\boldsymbol{\zeta} \in \mathbb{H}^1(\Omega)$ with $\mathbf{div}\boldsymbol{\zeta} \in \mathbf{H}^m(\Omega)$, $0 \le m \le k+1$, there holds

$$\left\|\,\mathbf{div}(\boldsymbol{\zeta} - \Pi_h^k(\boldsymbol{\zeta})\,\right\|_{0,T} \le C h_T^m |\,\mathbf{div}\boldsymbol{\zeta}\,|_{m,T} \quad \forall\, T \in \mathcal{T}_h\,, \tag{3.20}$$

iii) there exists $C > 0$ such that for each $\boldsymbol{\zeta} \in \mathbb{H}^1(\Omega)$ there holds

$$\left\| \boldsymbol{\zeta}\boldsymbol{\nu} - \Pi_h^k(\boldsymbol{\zeta})\boldsymbol{\nu} \right\|_{0,e} \leq C h_e^{1/2} \|\boldsymbol{\zeta}\|_{1,T_e} \quad \forall\, e \in \mathcal{E}_h(\Gamma)\,, \tag{3.21}$$

where T_e is the element of $\mathcal{T}_h$ having e as an edge.

Proof. See [5, Section III.3.3], [13, Section 3.4.4]. □

Lemma 3.6. *Let $X_h = \left\{ v_h \in C(\bar{\Omega}) : \ v_h\big|_T \in P_1(T) \quad \forall\, T \in \mathcal{T}_h \right\}$, and let $I_h : \mathrm{H}^1(\Omega) \to X_h$ be the usual Clément interpolation operator. Then, there exists $C > 0$ such that,*

$$\|\, v - I_h v \,\|_{0,T} \leq C h_T |\, v \,|_{1,\Delta(T)} \quad \forall\; T \in \mathcal{T}_h, \tag{3.22}$$

and

$$\|\, v - I_h v \,\|_{0,e} \leq C h_e^{1/2} \|\, v \,\|_{1,\Delta(e)} \quad \forall\; e \in \mathcal{E}_h, \tag{3.23}$$

where $\Delta(T)$ and $\Delta(e)$ are the unions of all elements intersecting T and e, respectively.

Proof. See [8]. □

Lemma 3.7 (Helmholtz Decomposition)**.** *For each $\boldsymbol{\tau} \in \mathbb{H}_0(\mathbf{div};\Omega)$, there exists $\mathbf{z} \in \mathbf{H}^2(\Omega)$ and $\boldsymbol{\phi} \in \mathbf{H}^1(\Omega)$ such that*

$$\boldsymbol{\tau} = \nabla \mathbf{z} + \underline{\mathbf{curl}}\, \boldsymbol{\phi} \ \text{ in } \Omega, \quad \text{and} \quad \|\, \mathbf{z} \,\|_{2,\Omega} + \|\, \boldsymbol{\phi} \,\|_{1,\Omega} \leq C \|\, \boldsymbol{\tau} \,\|_{\mathbf{div};\Omega}. \tag{3.24}$$

Proof. See [17, Lemma 3.7]. □

Therefore, owing to the previous decomposition, $\mathcal{R}^{\mathtt{m}}$ can be rewritten as follows.

Lemma 3.8. *Given $\boldsymbol{\tau} \in \mathbb{H}_0(\mathbf{div};\Omega)$, let $(\mathbf{z},\boldsymbol{\phi}) \in \mathbf{H}^2(\Omega) \times \mathbf{H}^1(\Omega)$ be the components of its associated Helmholtz decomposition. Then, there holds*

$$\mathcal{R}^{\mathtt{m}}(\boldsymbol{\tau}) = \mathcal{R}^{\mathtt{m}}_1(\nabla \mathbf{z}) + \mathcal{R}^{\mathtt{m}}_2(\underline{\mathbf{curl}}\, \boldsymbol{\phi}), \tag{3.25}$$

where

$$\begin{aligned} \mathcal{R}^{\mathtt{m}}_1(\nabla \mathbf{z}) = & \int_\Omega \Big\{ \mathbf{e}(\mathbf{u}_h) - \mu(\varphi_h)^{-1} (\mathbf{u}_h \otimes \mathbf{u}_h + \boldsymbol{\sigma}_h)^{\mathtt{d}} \Big\} : \nabla \mathbf{z} - \int_\Omega \Big\{ \boldsymbol{\gamma}_h - \boldsymbol{\omega}(\mathbf{u}_h) \Big\} : \nabla \mathbf{z} \\ & + \langle\, (\nabla \mathbf{z})\boldsymbol{\nu}, \mathbf{u}_D - \mathbf{u}_h \,\rangle_\Gamma - \kappa_2 \int_\Omega \Big\{ \mathbf{div}\, \boldsymbol{\sigma}_h + \varphi_h \mathbf{g} \Big\} \cdot \mathbf{div}\,(\nabla \mathbf{z}), \end{aligned} \tag{3.26}$$

and

$$\mathcal{R}^{\mathtt{m}}_2(\underline{\mathbf{curl}}\, \boldsymbol{\phi}) = -\int_\Omega \Big\{ \boldsymbol{\gamma}_h + \mu(\varphi_h)^{-1} (\mathbf{u}_h \otimes \mathbf{u}_h + \boldsymbol{\sigma}_h) \Big\} : \underline{\mathbf{curl}}\, \boldsymbol{\phi} + \langle\, (\underline{\mathbf{curl}}\, \boldsymbol{\phi})\boldsymbol{\nu}, \mathbf{u}_D \,\rangle_\Gamma. \tag{3.27}$$

Proof. Let $\boldsymbol{\tau} \in \mathbb{H}_0(\mathbf{div};\Omega)$. According to the definition of $\mathcal{R}^{\mathtt{m}}$ (cf. (3.6)) and considering the Helmholtz decomposition of $\boldsymbol{\tau}$ we get

$$\begin{aligned} \mathcal{R}^{\mathtt{m}}(\boldsymbol{\tau}) = & -\kappa_2 \int_\Omega \varphi_h \mathbf{g} \cdot \mathbf{div}\,(\nabla \mathbf{z}) + \langle\, (\nabla \mathbf{z})\boldsymbol{\nu}, \mathbf{u}_D \,\rangle_\Gamma + \langle\, (\underline{\mathbf{curl}}\, \boldsymbol{\phi})\boldsymbol{\nu}, \mathbf{u}_D \,\rangle_\Gamma - \int_\Omega \mu(\varphi_h)^{-1} \boldsymbol{\sigma}_h^{\mathtt{d}} : \nabla \mathbf{z} \\ & - \int_\Omega \mu(\varphi_h)^{-1} \boldsymbol{\sigma}_h^{\mathtt{d}} : \underline{\mathbf{curl}}\, \boldsymbol{\phi} - \int_\Omega \mathbf{u}_h \cdot \mathbf{div}\,(\nabla \mathbf{z}) - \kappa_2 \int_\Omega \mathbf{div}\, \boldsymbol{\sigma}_h \cdot \mathbf{div}\,(\nabla \mathbf{z}) \\ & - \int_\Omega \boldsymbol{\gamma}_h : \nabla \mathbf{z} - \int_\Omega \boldsymbol{\gamma}_h : \underline{\mathbf{curl}}\, \boldsymbol{\phi} - \int_\Omega \mu(\varphi_h)^{-1} (\mathbf{u}_h \otimes \mathbf{u}_h)^{\mathtt{d}} : \nabla \mathbf{z} \\ & - \int_\Omega \mu(\varphi_h)^{-1} (\mathbf{u}_h \otimes \mathbf{u}_h)^{\mathtt{d}} : \underline{\mathbf{curl}}\, \boldsymbol{\phi}, \end{aligned} \tag{3.28}$$

Then, as recommended by [9], we use the identity

$$-\int_\Omega \mathbf{u}_h \cdot \mathbf{div}\,(\nabla \mathbf{z}) + \langle\,(\nabla\mathbf{z})\boldsymbol{\nu}, \mathbf{u}_h\,\rangle_\Gamma = \int_\Omega \nabla\mathbf{u}_h : \nabla\mathbf{z} = \int_\Omega \mathbf{e}(\mathbf{u}_h) : \nabla\mathbf{z} + \int_\Omega \boldsymbol{\omega}(\mathbf{u}_h) : \nabla\mathbf{z},$$

in the sixth term of the right-hand side of (3.28) to obtain

$$\begin{aligned}\mathcal{R}^{\mathtt{m}}(\boldsymbol{\tau}) = \int_\Omega \Big\{\mathbf{e}(\mathbf{u}_h) - \mu(\varphi_h)^{-1}(\mathbf{u}_h\otimes\mathbf{u}_h + \boldsymbol{\sigma})^{\mathtt{d}}\Big\} : \nabla\mathbf{z} - \int_\Omega \Big\{\gamma_h - \boldsymbol{\omega}(\mathbf{u}_h)\Big\} : \nabla\mathbf{z} \\ + \langle\,(\nabla\mathbf{z})\boldsymbol{\nu}, \mathbf{u}_D - \mathbf{u}_h\,\rangle - \kappa_2 \int_\Omega \Big\{\mathbf{div}\,\boldsymbol{\sigma}_h + \varphi_h\mathbf{g}\Big\}\cdot\mathbf{div}\,(\nabla\mathbf{z}) \\ - \int_\Omega \Big\{\gamma_h + \mu(\varphi_h)^{-1}(\mathbf{u}_h\otimes\mathbf{u}_h + \boldsymbol{\sigma}_h)^{\mathtt{d}}\Big\} : \underline{\mathbf{curl}}\,\boldsymbol{\phi} + \langle\,(\underline{\mathbf{curl}}\,\boldsymbol{\phi})\boldsymbol{\nu}, \mathbf{u}_D\,\rangle_\Gamma,\end{aligned}$$

which corresponds to (3.25), thus concluding this way the proof. □

Hence, we can now bound $\|\,\mathcal{R}^{\mathtt{m}}\,\|$ by bounding the norms of the just introduced functionals $\mathcal{R}_1^{\mathtt{m}}$ and $\mathcal{R}_2^{\mathtt{m}}$, and using the stability result for the Helmholtz decomposition. Additionally for the estimation of $\|\,\mathcal{R}^{\mathtt{m}}\,\|$, according to (3.18), we can pick $\boldsymbol{\tau}_h$ as

$$\boldsymbol{\tau}_h^{\mathcal{R}} := \Pi_h^k(\nabla\mathbf{z}) + \underline{\mathbf{curl}}\,(\mathbf{I}_h\boldsymbol{\phi}) + c\mathbb{I}, \quad \text{with } c\in R \text{ such that } \int_\Omega \mathrm{tr}\big(\boldsymbol{\tau}_h^{\mathcal{R}}\big) = 0\,, \tag{3.29}$$

where $\mathbf{I}_h$ denotes the Clément interpolation operator I_h acting component-wise. Notice that, from the definition of $\mathcal{R}^{\mathtt{m}}$ and the compatibility condition (2.3), there holds $\mathcal{R}^{\mathtt{m}}(c\mathbb{I}) = 0$, whence

$$\mathcal{R}^{\mathtt{m}}(\boldsymbol{\tau} - \boldsymbol{\tau}_h^{\mathcal{R}}) = \mathcal{R}_1^{\mathtt{m}}(\nabla\mathbf{z} - \Pi_h^k(\nabla\mathbf{z})) + \mathcal{R}_2^{\mathtt{m}}(\underline{\mathbf{curl}}\,(\boldsymbol{\phi} - \mathbf{I}_h\boldsymbol{\phi})), \tag{3.30}$$

and so the reason why the Helmholtz decomposition in Lemma 3.7 is introduced. For the first term in (3.30), we have the following.

Lemma 3.9. *There exists a positive constant $\bar{C}_3$, independent of h, such that*

$$\begin{aligned}|\mathcal{R}_1^{\mathtt{m}}(\nabla\mathbf{z} - \Pi_h^k(\nabla\mathbf{z}))| \le \bar{C}_3\Big\{\sum_{T\in\mathcal{T}_h} h_T^2\|\,\mathbf{e}(\mathbf{u}_h) - \mu(\varphi_h)^{-1}(\mathbf{u}_h\otimes\mathbf{u}_h + \boldsymbol{\sigma}_h)^{\mathtt{d}}\,\|_{0,T}^2 \\ + \sum_{T\in\mathcal{T}_h} h_T^2\|\,\gamma_h - \boldsymbol{\omega}(\mathbf{u}_h)\,\|_{0,T}^2 + \sum_{T\in\mathcal{T}_h}\|\,\mathrm{div}\,\boldsymbol{\sigma}_h + \varphi_h\mathbf{g}\,\|_{0,T}^2 \\ + \sum_{e\in\mathcal{E}_h(\Gamma)} h_e\|\,\mathbf{u}_D - \mathbf{u}_h\,\|_{0,e}^2\Big\}^{1/2}\|\,\boldsymbol{\tau}\,\|_{\mathbf{div};\Omega}\,.\end{aligned} \tag{3.31}$$

Proof. Let us consider each term in the definition of $\mathcal{R}_1^{\mathtt{m}}$ (cf. (3.26)) separately. Applying the Cauchy-Schwarz inequality and the approximation property (3.19), we get

$$\begin{aligned}\Big|\int_\Omega \Big\{\mathbf{e}(\mathbf{u}_h) - \mu(\varphi_h)^{-1}(\mathbf{u}_h\otimes\mathbf{u}_h + \boldsymbol{\sigma}_h)^{\mathtt{d}}\Big\} : \Big\{\nabla\mathbf{z} - \Pi_h^k(\nabla\mathbf{z})\Big\}\Big| \\ \le \sum_{T\in\mathcal{T}_h} Ch_T\|\,\mathbf{e}(\mathbf{u}_h) - \mu(\varphi_h)^{-1}(\mathbf{u}_h\otimes\mathbf{u}_h + \boldsymbol{\sigma}_h)^{\mathtt{d}}\,\|_{0,T}|\,\nabla\mathbf{z}\,|_{1,T}.\end{aligned}$$

Similarly,

$$\Big|\int_\Omega \Big\{\gamma_h - \boldsymbol{\omega}(\mathbf{u}_h)\Big\} : \Big\{\nabla\mathbf{z} - \Pi_h^k(\nabla\mathbf{z})\Big\}\Big| \le \sum_{T\in\mathcal{T}_h} Ch_T\|\,\gamma_h - \boldsymbol{\omega}(\mathbf{u}_h)\,\|_{0,T}|\,\nabla\mathbf{z}\,|_{1,T}.$$

For the next term, we now consider the approximation property (3.20) to obtain

$$\left| -\kappa_2 \int_\Omega \Big\{ \mathbf{div}\,\boldsymbol{\sigma}_h + \varphi_h \mathbf{g} \Big\} \cdot \mathbf{div}\,(\nabla \mathbf{z} - \Pi_h^k(\nabla \mathbf{z})) \right| \leq \sum_{T\in\mathcal{T}_h} C \| \,\mathbf{div}\,\boldsymbol{\sigma}_h + \varphi_h \mathbf{g}\,\|_{0,T} \|\,\mathbf{div}\,(\nabla\mathbf{z})\,\|_{0,T},$$

and the bound for the remaining term can be obtained thanks to the approximation property (3.21),

$$\left| \Big\langle (\nabla \mathbf{z})\boldsymbol{\nu} - \Pi_h^k(\nabla \mathbf{z})\boldsymbol{\nu}, \mathbf{u}_D - \mathbf{u}_h \Big\rangle_\Gamma \right| \leq \sum_{e\in\mathcal{E}_h(\Gamma)} C h_e^{1/2} \|\,\mathbf{u}_D - \mathbf{u}_h\,\|_{0,e} |\,\nabla\mathbf{z}\,|_{1,T_e}.$$

Hence, by summing the last four inequalities, the result (3.31) comes as a consequence of the stability of the Helmholtz decomposition (cf. (3.24)) and the fact that $\mathbf{div}\,(\nabla\mathbf{z}) = \mathbf{div}\,\boldsymbol{\tau}$. □

On the other hand, the estimation for the second term in (3.30) requires an additional regularity of the boundary data $\mathbf{u}_D$.

Lemma 3.10. *Assume that* $\mathbf{u}_D \in \mathbf{H}^1(\Gamma)$*. Then, there exists a constant* $\bar{C}_4 > 0$ *independent of* h *such that*

$$\begin{aligned} |\mathcal{R}_2^{\mathtt{m}}(\underline{\mathbf{curl}}\,(\boldsymbol{\phi} - \mathbf{I}_h\boldsymbol{\phi}))| \leq \bar{C}_4 \Bigg\{ & \sum_{T\in\mathcal{T}_h} h_T^2 \|\,\mathrm{curl}\,\{\boldsymbol{\gamma}_h + \mu(\varphi_h)^{-1}(\mathbf{u}_h\otimes\mathbf{u}_h + \boldsymbol{\sigma}_h)^{\mathtt{d}}\}\,\|_{0,T}^2 \\ & + \sum_{e\in\mathcal{E}_h(\Omega)} h_e \|\,[\![\{\boldsymbol{\gamma}_h + \mu(\varphi_h)^{-1}(\mathbf{u}_h\otimes\mathbf{u}_h + \boldsymbol{\sigma}_h)^{\mathtt{d}}\}\boldsymbol{s}]\!]\,\|_{0,e}^2 \\ & + \sum_{e\in\mathcal{E}_h(\Gamma)} h_e \left\|\,\{\boldsymbol{\gamma}_h + \mu(\varphi_h)^{-1}(\mathbf{u}_h\otimes\mathbf{u}_h + \boldsymbol{\sigma}_h)^{\mathtt{d}}\}\boldsymbol{s} - \frac{\mathrm{d}\mathbf{u}_D}{\mathrm{d}\boldsymbol{s}}\,\right\|_{0,e}^2 \Bigg\}^{1/2} \|\,\boldsymbol{\tau}\,\|_{\mathbf{div};\Omega}. \end{aligned} \tag{3.32}$$

Proof. We recall from [17, Lemma 3.8] the following integration-by-parts formula on the boundary,

$$\langle\, (\underline{\mathbf{curl}}\,\boldsymbol{\psi})\boldsymbol{\nu}, \boldsymbol{\chi}\,\rangle_\Gamma = -\left\langle \frac{\mathrm{d}\boldsymbol{\chi}}{\mathrm{d}\boldsymbol{s}}, \boldsymbol{\psi} \right\rangle_\Gamma \quad \forall\, \boldsymbol{\psi}, \boldsymbol{\chi} \in \mathbf{H}^1(\Omega).$$

Then, applying this to $\boldsymbol{\psi} = \boldsymbol{\phi} - \mathbf{I}_h\boldsymbol{\phi}$ and to a trace lifting $\boldsymbol{\chi}$ of $\mathbf{u}_D$, plus a local integration by parts, we have from (3.27) that

$$\begin{aligned} \mathcal{R}_2^{\mathtt{m}}(\underline{\mathbf{curl}}\,(\boldsymbol{\phi} - \mathbf{I}_h\boldsymbol{\phi})) = -\sum_{T\in\mathcal{T}_h} \Bigg\{ & \int_T \mathrm{curl}\,\{\boldsymbol{\gamma}_h + \mu(\varphi_h)^{-1}(\mathbf{u}_h\otimes\mathbf{u}_h + \boldsymbol{\sigma}_h)^{\mathtt{d}}\} \cdot (\boldsymbol{\phi} - \mathbf{I}_h\boldsymbol{\phi}) \\ & + \sum_{e\subseteq\partial T} \int_e \{\boldsymbol{\gamma}_h + \mu(\varphi_h)^{-1}(\mathbf{u}_h\otimes\mathbf{u}_h + \boldsymbol{\sigma}_h)^{\mathtt{d}}\}\boldsymbol{s}\cdot(\boldsymbol{\phi} - \mathbf{I}_h\boldsymbol{\phi}) \Bigg\} - \left\langle \frac{\mathrm{d}\mathbf{u}_D}{\mathrm{d}\boldsymbol{s}}, \boldsymbol{\phi} - \mathbf{I}_h\boldsymbol{\phi} \right\rangle_\Gamma. \end{aligned}$$

Moreover, we make the differentiation between the integration over the edges in the interior and in the boundary of the domain. Since we are assuming that $\dfrac{\mathrm{d}\mathbf{u}_D}{\mathrm{d}\boldsymbol{s}} \in \mathbf{L}^2(\Gamma)$, the following can be written,

$$\begin{aligned} \mathcal{R}_2^{\mathtt{m}}(\underline{\mathbf{curl}}\,(\boldsymbol{\phi} - \mathbf{I}_h\boldsymbol{\phi})) = & -\sum_{T\in\mathcal{T}_h} \int_T \mathrm{curl}\,\{\boldsymbol{\gamma}_h + \mu(\varphi_h)^{-1}(\mathbf{u}_h\otimes\mathbf{u}_h + \boldsymbol{\sigma}_h)^{\mathtt{d}}\} \cdot (\boldsymbol{\phi} - \mathbf{I}_h\boldsymbol{\phi}) \\ & + \sum_{e\in\mathcal{E}_h(\Omega)} \int_e [\![\{\boldsymbol{\gamma}_h + \mu(\varphi_h)^{-1}(\mathbf{u}_h\otimes\mathbf{u}_h + \boldsymbol{\sigma}_h)^{\mathtt{d}}\}\boldsymbol{s}]\!] \cdot (\boldsymbol{\phi} - \mathbf{I}_h\boldsymbol{\phi}) \\ & + \sum_{e\in\mathcal{E}_h(\Gamma)} \int_e \left\{ \{\boldsymbol{\gamma}_h + \mu(\varphi_h)^{-1}(\mathbf{u}_h\otimes\mathbf{u}_h + \boldsymbol{\sigma}_h)^{\mathtt{d}}\}\boldsymbol{s} - \frac{\mathrm{d}\mathbf{u}_D}{\mathrm{d}\boldsymbol{s}} \right\} \cdot (\boldsymbol{\phi} - \mathbf{I}_h\boldsymbol{\phi}). \end{aligned}$$

Hence, applying the Cauchy-Schwarz inequality to this expression, and the approximation properties of the Clément interpolant (cf. (3.22) - (3.23)), we get

$$
\begin{aligned}
|\mathcal{R}_2^{\mathtt{m}}(\underline{\mathbf{curl}}\,(\boldsymbol{\phi}-\mathbf{I}_h\boldsymbol{\phi}))| \le & \sum_{T\in\mathcal{T}_H} C h_T \big\| \operatorname{curl}\left\{\boldsymbol{\gamma}_h + \mu(\varphi_h)^{-1}(\mathbf{u}_h\otimes\mathbf{u}_h+\boldsymbol{\sigma}_h)^{\mathtt{d}}\right\} \big\|_{0,T} \| \boldsymbol{\phi} \|_{1,\Delta(T)} \\
& + \sum_{e\in\mathcal{E}_h(\Omega)} C h_e^{1/2} \big\| [\![\{\boldsymbol{\gamma}_h + \mu(\varphi_h)^{-1}(\mathbf{u}_h\otimes\mathbf{u}_h+\boldsymbol{\sigma}_h)^{\mathtt{d}}\}\boldsymbol{s}]\!] \big\|_{0,e} \| \boldsymbol{\phi} \|_{1,\Delta(e)} \\
& + \sum_{e\in\mathcal{E}_h(\Gamma)} C h_e^{1/2} \left\| \{\boldsymbol{\gamma}_h + \mu(\varphi_h)^{-1}(\mathbf{u}_h\otimes\mathbf{u}_h+\boldsymbol{\sigma}_h)^{\mathtt{d}}\}\boldsymbol{s} - \frac{\mathrm{d}\mathbf{u}_D}{\mathrm{d}\boldsymbol{s}} \right\|_{0,e} \| \boldsymbol{\phi} \|_{1,\Delta(e)},
\end{aligned}
$$

thus obtaining the result (3.32) by considering the shape-regularity of the mesh and the stability of the Helmholtz decomposition. $\square$

Following the last two lemmas, the estimate for $\| \mathcal{R}^{\mathtt{m}} \|$ becomes straightforward.

Lemma 3.11. *Assume that* $\mathbf{u}_D \in \mathbf{H}^1(\Gamma)$. *Then, there exists* $\bar{C} > 0$ *independent of* h *such that*

$$
\begin{aligned}
\| \mathcal{R}^{\mathtt{m}} \| \le \bar{C} \Bigg\{ & \sum_{T\in\mathcal{T}_h} \Big(h_T^2 \| \mathbf{e}(\mathbf{u}_h) - \mu(\varphi_h)^{-1}(\mathbf{u}_h\otimes\mathbf{u}_h+\boldsymbol{\sigma}_h)^{\mathtt{d}} \|_{0,T}^2 + h_T^2 \| \boldsymbol{\gamma}_h - \boldsymbol{\omega}(\mathbf{u}_h) \|_{0,T}^2 \\
& + \| \operatorname{div}\boldsymbol{\sigma}_h - \varphi_h \mathbf{g} \|_{0,T}^2 + h_T^2 \| \operatorname{curl}\left\{\boldsymbol{\gamma}_h + \mu(\varphi_h)^{-1}(\mathbf{u}_h\otimes\mathbf{u}_h+\boldsymbol{\sigma}_h)^{\mathtt{d}}\right\} \|_{0,T}^2 \Big) \\
& + \sum_{e\in\mathcal{E}_h(\Omega)} h_e \| [\![\{\boldsymbol{\gamma}_h + \mu(\varphi_h)^{-1}(\mathbf{u}_h\otimes\mathbf{u}_h+\boldsymbol{\sigma}_h)^{\mathtt{d}}\}\boldsymbol{s}]\!] \|_{0,e}^2 \\
& + \sum_{e\in\mathcal{E}_h(\Gamma)} h_e \left(\left\| \{\boldsymbol{\gamma}_h + \mu(\varphi_h)^{-1}(\mathbf{u}_h\otimes\mathbf{u}_h+\boldsymbol{\sigma}_h)^{\mathtt{d}}\}\boldsymbol{s} - \frac{\mathrm{d}\mathbf{u}_D}{\mathrm{d}\boldsymbol{s}} \right\|_{0,e}^2 + \| \mathbf{u}_D - \mathbf{u}_h \|_{0,e}^2 \right) \Bigg\}^{1/2}.
\end{aligned}
$$

Proof. We go back to our definition of $\| \mathcal{R}^{\mathtt{m}} \|$ in (3.18), and considering the choice of $\boldsymbol{\tau}_h$ made in (3.29), the result comes from (3.30) by adding the estimates in the previous two lemmas, i.e., (3.31) and (3.32), and an application of the classical Cauchy-Schwarz inequality. $\square$

The estimation of $\| \mathcal{R}^{\mathtt{e}} \|$ proceeds in a similar way. In fact, using the definition of this norm in (3.18) and choosing ψ_h as $\psi_h^{\mathcal{R}} = I_h\psi$, the approximation properties of I_h (cf. Lemma 3.6) allow to prove the result we cite next.

Lemma 3.12. *There exists a positive constant* $\bar{C} > 0$ *independent of* h *and* $\widetilde{h}$ *such that*

$$
\begin{aligned}
\| \mathcal{R}^{\mathtt{e}} \| \le \bar{C} \Bigg\{ & \sum_{T\in\mathcal{T}_h} h_T^2 \| \operatorname{div}(\mathbb{K}\nabla\varphi_h) - \mathbf{u}_h\cdot\nabla\varphi_h \|_{0,T}^2 \\
& + \sum_{e\in\mathcal{E}_h(\Omega)} h_e \| [\![\mathbb{K}\nabla\varphi_h\cdot\boldsymbol{\nu}]\!] \|_{0,e}^2 + \sum_{e\in\mathcal{E}_h(\Gamma)} h_e \| \lambda_{\widetilde{h}} + \mathbb{K}\nabla\varphi_h\cdot\boldsymbol{\nu} \|_{0,e}^2 \Bigg\}^{1/2}
\end{aligned}
$$

Proof. [9, Lemma 3.12]. $\square$

Therefore, it can be seen that the reliability of the estimator $\boldsymbol{\theta}$ introduced in (3.1) is a consequence of Lemmas 3.4, 3.11 and 3.12. Notice that we have discarded the terms

$$h_T^2 \| \mathbf{e}(\mathbf{u}_h) - \mu(\varphi_h)^{-1}(\mathbf{u}_h \otimes \mathbf{u}_h + \boldsymbol{\sigma}_h)^{\mathtt{d}} \|_{0,T}^2, \quad h_T^2 \| \boldsymbol{\gamma}_h - \boldsymbol{\omega}(\mathbf{u}_h) \|_{0,T}^2,$$
$$\| \operatorname{div} \boldsymbol{\sigma}_h - \varphi_h \mathbf{g} \|_{0,T}^2 \quad \text{and} \quad h_e \| \mathbf{u}_D - \mathbf{u}_h \|_{0,e}^2,$$

since they are dominated by linear versions of them already present in Lemma 3.4.

3.3 Efficiency

This section will be focused in the proof of the following result.

Theorem 3.13. *Let $(\vec{\boldsymbol{\sigma}}, (\varphi, \lambda))$ and $(\vec{\boldsymbol{\sigma}}_h, (\varphi_h, \lambda_{\widetilde{h}}))$ be solutions to (2.6) and (2.22), respectively, and suppose for simplicity that $\mathbf{u}_D$ and $\mathbb{K}$ are piecewise polynomials. In addition, assume that there exists $\varepsilon \in (0,1)$ such that $\mathbf{u}_D \in \mathbf{H}^{1/2+\varepsilon}(\Gamma)$, $\boldsymbol{\sigma} \in \mathbb{H}^{\varepsilon}(\Omega)$, and the regularity hypothesis (3.3) holds. Furthermore, suppose that the partition on Γ inherited from $\mathcal{T}_h$ is quasi-uniform, and that each edge of $\mathcal{E}_h(\Gamma)$ is contained in one of the elements of the independent partition of Γ defining $\mathrm{H}_{\widetilde{h}}^{\lambda}$. Then $\boldsymbol{\theta}$ is an efficient estimator, i.e., there exists a positive constant C_{eff}, depending on physical and stabilization parameters, but independent of h and $\widetilde{h}$, such that*

$$C_{\text{eff}}\ \boldsymbol{\theta} \le \| (\vec{\boldsymbol{\sigma}}, (\varphi, \lambda)) - (\vec{\boldsymbol{\sigma}}_h, (\varphi_h, \lambda_{\widetilde{h}})) \|. \tag{3.33}$$

We begin with an estimate that will be useful in the upcoming analysis.

Lemma 3.14. *Assume the same hypotheses of Theorem 3.13. Then there exists $\widetilde{C} > 0$ depending on the given data, but independent of h, such that*

$$\| \mu(\varphi)^{-1}(\mathbf{u} \otimes \mathbf{u} + \boldsymbol{\sigma})^{\mathtt{d}} - \mu(\varphi_h)^{-1}(\mathbf{u}_h \otimes \mathbf{u}_h + \boldsymbol{\sigma}_h)^{\mathtt{d}} \|_{0,\Omega}^2 \le \widetilde{C} \| (\boldsymbol{\sigma}, \mathbf{u}, \varphi) - (\boldsymbol{\sigma}_h, \mathbf{u}_h, \varphi_h) \|^2. \tag{3.34}$$

Proof. Adding and substracting the term $\mu(\varphi_h)^{-1}(\mathbf{u} \otimes \mathbf{u} + \boldsymbol{\sigma})^{\mathtt{d}}$ in the left-hand side of the previous inequality, we have

$$\begin{aligned} &\| \mu(\varphi)^{-1}(\mathbf{u} \otimes \mathbf{u} + \boldsymbol{\sigma})^{\mathtt{d}} - \mu(\varphi_h)^{-1}(\mathbf{u}_h \otimes \mathbf{u}_h + \boldsymbol{\sigma}_h)^{\mathtt{d}} \|_{0,\Omega}^2 \\ &\quad \le 2 \left\| \frac{\mu(\varphi_h) - \mu(\varphi)}{\mu(\varphi)\mu(\varphi_h)} (\mathbf{u} \otimes \mathbf{u} + \boldsymbol{\sigma})^{\mathtt{d}} \right\|_{0,\Omega}^2 \\ &\quad + 2 \| \mu(\varphi_h)^{-1} \big[(\boldsymbol{\sigma} - \boldsymbol{\sigma}_h)^{\mathtt{d}} + (\mathbf{u} \otimes \mathbf{u} - \mathbf{u}_h \otimes \mathbf{u}_h) \big] \|_{0,\Omega}^2 . \end{aligned} \tag{3.35}$$

For the first term in the right-hand side of (3.35), we follow the same steps realized while bounding the norm of the operator $\mathcal{S}$ in (3.14) and use the Lipschitz continuity and boundedness of μ, the continuous injections of $\mathrm{H}^1(\Omega)$ into $\mathrm{L}^{2/\varepsilon}(\Omega)$, $\mathrm{L}^4(\Omega)$ and $\mathrm{L}^8(\Omega)$, of $\mathrm{H}^{\varepsilon}(\Omega)$ into $\mathrm{L}^{2/(1-\varepsilon)}$, and the further regularity assumption in (3.3) to show that

$$\begin{aligned} \left\| \frac{\mu(\varphi_h) - \mu(\varphi)}{\mu(\varphi)\mu(\varphi_h)} (\mathbf{u} \otimes \mathbf{u} + \boldsymbol{\sigma})^{\mathtt{d}} \right\|_{0,\Omega}^2 &\le \frac{2L_\mu^2}{\mu_1^4} \Big\{ \| (\varphi_h - \varphi)(\mathbf{u} \otimes \mathbf{u}) \|_{0,\Omega}^2 + \| (\varphi_h - \varphi)\boldsymbol{\sigma} \|_{0,\Omega}^2 \Big\} \\ &\le \frac{2L_\mu^2}{\mu_1^4} \Big\{ C_i^2 \| \varphi - \varphi_h \|_{1,\Omega}^2 \| \mathbf{u} \|_{1,\Omega}^4 + C_\varepsilon^2 \widetilde{C}_\varepsilon^2 \| \varphi - \varphi_h \|_{1,\Omega}^2 \| \boldsymbol{\sigma} \|_{\varepsilon,\Omega}^2 \Big\} \\ &= \frac{2L_\mu^2}{\mu_1^4} \Big\{ C_i^2 \| \mathbf{u} \|_{1,\Omega}^4 + C_\varepsilon^2 \widetilde{C}_\varepsilon^2 \| \boldsymbol{\sigma} \|_{\varepsilon,\Omega}^2 \Big\} \| \varphi - \varphi_h \|_{1,\Omega}^2 . \end{aligned}$$

Then, for the second one

$$\begin{aligned}
&\| \mu(\varphi_h)^{-1}\big[(\boldsymbol{\sigma}-\boldsymbol{\sigma}_h)^{\mathtt{d}} + (\mathbf{u}\otimes\mathbf{u}-\mathbf{u}_h\otimes\mathbf{u}_h)\big] \|_{0,\Omega}^2 \\
&\quad\le \frac{2}{\mu_1^2}\| \boldsymbol{\sigma}-\boldsymbol{\sigma}_h \|_{0,\Omega}^2 + \frac{2}{\mu_1^2}\| (\mathbf{u}+\mathbf{u}_h)\otimes(\mathbf{u}-\mathbf{u}_h) \|_{0,\Omega}^2 \\
&\quad\le \frac{2}{\mu_1^2}\| \boldsymbol{\sigma}-\boldsymbol{\sigma}_h \|_{\mathbf{div};\Omega}^2 + \frac{2\widetilde{C}_i^2}{\mu_1^2}\| \mathbf{u}+\mathbf{u}_h \|_{1,\Omega}^2\| \mathbf{u}-\mathbf{u}_h \|_{1,\Omega}^2 \\
&\quad\le \left\{\frac{2}{\mu_1^2} + \frac{2\widetilde{C}_i}{\mu_1^2}\| \mathbf{u}+\mathbf{u}_h \|_{1,\Omega}^2\right\}\| (\boldsymbol{\sigma},\mathbf{u}) - (\boldsymbol{\sigma}_h,\mathbf{u}_h) \|^2 .
\end{aligned}$$

Hence, since $\| \mathbf{u} \|_{1,\Omega}$, $\| \mathbf{u}_h \|_{1,\Omega}$ and $\| \boldsymbol{\sigma} \|_{\varepsilon,\Omega}$ can be bounded by data using the estimates (2.15), (2.23) and (3.3), respectively, the sum of the last two inequalities gives the proof of (3.34). $\square$

Bounds like the one presented in the foregoing Lemma will appear frequently, and it also shows us one of the issues that arise when proving the local efficiency of the estimator $\boldsymbol{\theta}$: any continuous injection will have a boundedness constant that depends on the corresponding domain, in this case, each element of the triangulation, hence, a partial solution would be to consider the error terms in non-natural L^p norms (i.e, different to the original norms that one should consider according to the variational formulations). For this reason, we only focus in proving global efficiency estimates, as indeed needed for Theorem 3.13. We first address those terms in the definition of $\boldsymbol{\theta}$ (cf. (3.1)) that are not multiplied by a triangle-dependent term.

Lemma 3.15. *There exists $\widetilde{C}_1, \widetilde{C}_2 > 0$, both independent of h and $\widetilde{h}$, such that*

$$\| \varphi_D - \varphi_h \|_{1/2,\Gamma}^2 + \| \mathbf{u}_D - \mathbf{u}_h \|_{1/2,\Gamma}^2 \le \widetilde{C}_1\| (\mathbf{u},\varphi) - (\mathbf{u}_h,\varphi_h) \|^2, \tag{3.36}$$

and

$$\begin{aligned}
&\| \mathbf{e}(\mathbf{u}_h) - \mu(\varphi_h)^{-1}(\mathbf{u}_h\otimes\mathbf{u}_h + \boldsymbol{\sigma}_h)^{\mathtt{d}} \|_{0,\Omega}^2 + \| \mathbf{div}\,\boldsymbol{\sigma}_h + \varphi_h\mathbf{g} \|_{0,\Omega}^2 \\
&\qquad + \| \boldsymbol{\gamma}_h - \boldsymbol{\omega}(\mathbf{u}_h) \|_{0,\Omega}^2 + \| \boldsymbol{\sigma}_h - \boldsymbol{\sigma}_h^{\mathtt{t}} \|_{0,\Omega}^2 \le \widetilde{C}_2\| (\vec{\boldsymbol{\sigma}},\varphi) - (\vec{\boldsymbol{\sigma}}_h,\varphi_h) \|^2.
\end{aligned} \tag{3.37}$$

Proof. The first inequality is a mere consequence of the trace theorem, as $\varphi_D = \varphi\big|_\Gamma$ and $\mathbf{u}_D = \mathbf{u}\big|_\Gamma$. On the other hand, for the first term in (3.37), using that $\mathbf{e}(\mathbf{u}) - \mu(\varphi)^{-1}(\mathbf{u}\otimes\mathbf{u}+\boldsymbol{\sigma})^{\mathtt{d}} = 0$ in Ω, we see that

$$\begin{aligned}
&\| \mathbf{e}(\mathbf{u}_h) - \mu(\varphi_h)^{-1}(\mathbf{u}_h\otimes\mathbf{u}_h + \boldsymbol{\sigma}_h)^{\mathtt{d}} \|_{0,\Omega}^2 \\
&\qquad = \| \mathbf{e}(\mathbf{u}_h-\mathbf{u}) + \mu(\varphi)^{-1}(\mathbf{u}\otimes\mathbf{u}+\boldsymbol{\sigma})^{\mathtt{d}} - \mu(\varphi_h)^{-1}(\mathbf{u}_h\otimes\mathbf{u}_h+\boldsymbol{\sigma}_h)^{\mathtt{d}} \|_{0,\Omega}^2 \\
&\qquad \le 2\| \mathbf{e}(\mathbf{u}_h-\mathbf{u}) \|_{0,\Omega}^2 + 2\| \mu(\varphi_h)^{-1}(\mathbf{u}_h\otimes\mathbf{u}_h+\boldsymbol{\sigma}_h)^{\mathtt{d}} - \mu(\varphi)^{-1}(\mathbf{u}\otimes\mathbf{u}+\boldsymbol{\sigma})^{\mathtt{d}} \|_{0,\Omega}^2 \\
&\qquad \le 2\| \mathbf{u}-\mathbf{u}_h \|_{1,\Omega}^2 + 2\widetilde{C}\| (\boldsymbol{\sigma},\mathbf{u},\varphi) - (\boldsymbol{\sigma}_h,\mathbf{u}_h,\varphi_h) \|^2, \\
&\qquad \le C\| (\boldsymbol{\sigma},\mathbf{u},\varphi) - (\boldsymbol{\sigma}_h,\mathbf{u}_h,\varphi_h) \|^2 ,
\end{aligned} \tag{3.38}$$

where the second inequality comes from an application of Lemma 3.14. Analogously, using that $\mathbf{div}\,\boldsymbol{\sigma} + \varphi\mathbf{g} = 0$ in Ω, we have

$$\begin{aligned}
\| \mathbf{div}\,\boldsymbol{\sigma}_h + \varphi_h\mathbf{g} \|_{0,\Omega}^2 &= \| \mathbf{div}\,(\boldsymbol{\sigma}-\boldsymbol{\sigma}_h) + (\varphi-\varphi_h)\mathbf{g} \|_{0,\Omega}^2 \\
&\le 2\| \boldsymbol{\sigma}-\boldsymbol{\sigma}_h \|_{\mathbf{div};\Omega}^2 + 2\| \mathbf{g} \|_{\infty,\Omega}^2\| \varphi-\varphi_h \|_{1,\Omega}^2 \\
&\le C\| (\boldsymbol{\sigma},\varphi) - (\boldsymbol{\sigma}_h,\varphi_h) \|^2 .
\end{aligned} \tag{3.39}$$

For the third term, we use that $\boldsymbol{\gamma} = \boldsymbol{\omega}(\mathbf{u})$ in Ω to obtain

$$\begin{aligned} \| \boldsymbol{\gamma}_h - \boldsymbol{\omega}(\mathbf{u}_h) \|_{0,\Omega}^2 &= \| (\boldsymbol{\gamma} - \boldsymbol{\gamma}_h) - \boldsymbol{\omega}(\mathbf{u} - \mathbf{u}_h) \|_{0,\Omega}^2 \\ &\leq 2 \| \boldsymbol{\gamma} - \boldsymbol{\gamma}_h \|_{0,\Omega}^2 + 2 \| \mathbf{u} - \mathbf{u}_h \|_{1,\Omega}^2 \leq C \| (\mathbf{u}, \boldsymbol{\gamma}) - (\mathbf{u}_h, \boldsymbol{\gamma}_h) \|^2 , \end{aligned} \tag{3.40}$$

and for the last term in (3.37), since $\boldsymbol{\sigma}$ is, by definition, a symmetric tensor (cf. (2.4)) (and so is its $\mathbb{H}_0(\mathbf{div};\Omega)$-component), we have

$$\| \boldsymbol{\sigma}_h - \boldsymbol{\sigma}_h^{\mathtt{t}} \|_{0,\Omega}^2 = \| (\boldsymbol{\sigma} - \boldsymbol{\sigma}_h) - (\boldsymbol{\sigma} - \boldsymbol{\sigma}_h)^{\mathtt{t}} \|_{0,\Omega}^2 \leq C \| \boldsymbol{\sigma} - \boldsymbol{\sigma}_h \|_{\mathbf{div};\Omega}^2 . \tag{3.41}$$

Therefore, (3.37) follows after summing (3.38) - (3.41). □

Before moving on to the next terms, we recall from [16] the following result.

Lemma 3.16. *Let $\boldsymbol{\zeta}_h \in \mathbb{L}^2(\Omega)$ be a piecewise polynomial of degree $k \geq 0$ on each $T \in \mathcal{T}_h$. In addition, let $\boldsymbol{\zeta} \in \mathbb{L}^2(\Omega)$ be such that $\operatorname{curl} \boldsymbol{\zeta} = 0$ on each $T \in \mathcal{T}_h$. Then, there exists $C > 0$, independent of h, such that*

$$\| \operatorname{curl} \boldsymbol{\zeta}_h \|_{0,T} \leq C h_T^{-1} \| \boldsymbol{\zeta} - \boldsymbol{\zeta}_h \|_{0,T} \qquad \forall\, T \in \mathcal{T}_h . \tag{3.42}$$

Moreover, if $\operatorname{curl} \boldsymbol{\zeta} = 0$ in Ω, then there exists $C > 0$, independent of h, such that

$$\| [\![\boldsymbol{\zeta} \boldsymbol{s}]\!] \|_{0,e} \leq C h_e^{-1/2} \| \boldsymbol{\zeta} - \boldsymbol{\zeta}_h \|_{0,\omega_e} \qquad \forall\, e \in \mathcal{E}_h(\Omega) , \tag{3.43}$$

where ω_e is the union of the two elements of $\mathcal{T}_h$ sharing the edge e.

Proof. See [16, Lemmas 4.9, 4.10]. □

Having in mind these inequalities, the following can be proved.

Lemma 3.17. *There exists $\widetilde{C}_3$, independent of h and $\widetilde{h}$, such that*

$$\begin{aligned} &\sum_{T \in \mathcal{T}_h} h_T^2 \| \operatorname{curl} \left\{ \boldsymbol{\gamma}_h + \mu(\varphi_h)^{-1} (\mathbf{u}_h \otimes \mathbf{u}_h + \boldsymbol{\sigma}_h)^{\mathtt{d}} \right\} \|_{0,T}^2 \\ &\quad + \sum_{e \in \mathcal{E}_h(\Omega)} h_e \| [\![\big(\boldsymbol{\gamma}_h + \mu(\varphi_h)^{-1} (\mathbf{u}_h \otimes \mathbf{u}_h + \boldsymbol{\sigma}_h)^{\mathtt{d}} \big) \boldsymbol{s}]\!] \|_{0,e}^2 \leq \widetilde{C}_3 \| (\vec{\boldsymbol{\sigma}}, \varphi) - (\vec{\boldsymbol{\sigma}}_h, \varphi_h) \|^2 . \end{aligned} \tag{3.44}$$

Additionally, if $\mathbf{u}_D$ is piecewise polynomial, there exists $\widetilde{C}_4 > 0$ such that

$$\sum_{e \in \mathcal{E}_h(\Gamma)} h_e \left\| \big(\boldsymbol{\gamma}_h + \mu(\varphi_h)^{-1} (\mathbf{u}_h \otimes \mathbf{u}_h + \boldsymbol{\sigma}_h)^{\mathtt{d}} \big) \boldsymbol{s} - \frac{\mathrm{d}\mathbf{u}_D}{\mathrm{d}\boldsymbol{s}} \right\|_{0,e}^2 \leq \widetilde{C}_4 \| (\vec{\boldsymbol{\sigma}}, \varphi) - (\vec{\boldsymbol{\sigma}}_h, \varphi_h) \|^2 . \tag{3.45}$$

Proof. Applying Lemma 3.16 with $\boldsymbol{\zeta}_h = \boldsymbol{\gamma}_h + \mu(\varphi_h)^{-1} (\mathbf{u}_h \otimes \mathbf{u}_h + \boldsymbol{\sigma}_h)^{\mathtt{d}}$ and $\boldsymbol{\zeta} = \boldsymbol{\gamma} + \mu(\varphi)^{-1} (\mathbf{u} \otimes \mathbf{u} + \boldsymbol{\sigma})^{\mathtt{d}} = \nabla \mathbf{u}$ (whose curl vanishes both locally and globally), we obtain

$$\begin{aligned} &\| \operatorname{curl} \left\{ \boldsymbol{\gamma}_h + \mu(\varphi_h)^{-1} (\mathbf{u}_h \otimes \mathbf{u}_h + \boldsymbol{\sigma}_h)^{\mathtt{d}} \right\} \|_{0,T}^2 \\ &\qquad \leq C h_T^{-2} \| (\boldsymbol{\gamma} - \boldsymbol{\gamma}_h) + \mu(\varphi)^{-1} (\mathbf{u} \otimes \mathbf{u} + \boldsymbol{\sigma})^{\mathtt{d}} - \mu(\varphi_h)^{-1} (\mathbf{u}_h \otimes \mathbf{u}_h + \boldsymbol{\sigma}_h)^{\mathtt{d}} \|_{0,T}^2 \\ &\qquad \leq C h_T^{-2} \left\{ 2 \| \boldsymbol{\gamma} - \boldsymbol{\gamma}_h \|_{0,T}^2 + 2 \| \mu(\varphi)^{-1} (\mathbf{u} \otimes \mathbf{u} + \boldsymbol{\sigma})^{\mathtt{d}} - \mu(\varphi_h)^{-1} (\mathbf{u}_h \otimes \mathbf{u}_h + \boldsymbol{\sigma}_h)^{\mathtt{d}} \|_{0,T}^2 \right\} \end{aligned}$$

and

$$\| \, [\![\{\gamma_h + \mu(\varphi_h)^{-1}(\mathbf{u}_h \otimes \mathbf{u}_h + \boldsymbol{\sigma}_h)^{\mathtt{d}}\}\boldsymbol{s}]\!] \, \|^2_{0,e} \\ \le C h_e^{-1} \left\{ 2\| \, \boldsymbol{\gamma} - \boldsymbol{\gamma}_h \, \|^2_{0,\omega_e} + 2\| \, \mu(\varphi)^{-1}(\mathbf{u} \otimes \mathbf{u} + \boldsymbol{\sigma})^{\mathtt{d}} - \mu(\varphi_h)^{-1}(\mathbf{u}_h \otimes \mathbf{u}_h + \boldsymbol{\sigma}_h)^{\mathtt{d}} \, \|^2_{0,\omega_e} \right\}.$$

Thus, summing over all triangles and interior edges the last two inequalities, and then applying Lemma 3.14, we get (3.44). On the other hand, the proof of (3.45) begins with the same arguments as in [16, Lemma 4.15]. Indeed, the following local result can be obtained replacing the discrete tensor $\frac{1}{2\mu}\boldsymbol{\sigma}_h^{\mathtt{d}}$ by $\boldsymbol{\gamma}_h + \mu(\varphi_h)^{-1}(\mathbf{u}_h \otimes \mathbf{u}_h + \boldsymbol{\sigma}_h)^{\mathtt{d}}$ in the cited lemma,

$$h_e \left\| \, \big(\boldsymbol{\gamma}_h + \mu(\varphi_h)^{-1}(\mathbf{u}_h \otimes \mathbf{u}_h + \boldsymbol{\sigma}_h)^{\mathtt{d}}\big)\boldsymbol{s} - \frac{\mathrm{d}\mathbf{u}_D}{\mathrm{d}\boldsymbol{s}} \, \right\|^2_{0,e} \\ \le \widehat{C} \Big\{ \| \, (\boldsymbol{\gamma} - \boldsymbol{\gamma}_h) + \mu(\varphi)^{-1}(\mathbf{u} \otimes \mathbf{u} + \boldsymbol{\sigma})^{\mathtt{d}} - \mu(\varphi_h)^{-1}(\mathbf{u}_h \otimes \mathbf{u}_h + \boldsymbol{\sigma}_h)^{\mathtt{d}} \, \|^2_{0,T_e} \\ + h_e^2 \, \| \, \mathrm{curl} \, \{ \boldsymbol{\gamma}_h + \mu(\varphi_h)^{-1}(\mathbf{u}_h \otimes \mathbf{u}_h + \boldsymbol{\sigma}_h)^{\mathtt{d}} \} \, \|^2_{0,T_e} \Big\},$$

where T_e is the triangle to which the boundary edge e belongs. Then, summing over all boundary edges, using that $h_e \le h_{T_e}$, applying Lemma 3.14, and using (3.44), we arrive at

$$\sum_{e \in \mathcal{E}_h(\Gamma)} h_e \left\| \, \big(\boldsymbol{\gamma}_h + \mu(\varphi_h)^{-1}(\mathbf{u}_h \otimes \mathbf{u}_h + \boldsymbol{\sigma}_h)^{\mathtt{d}}\big)\boldsymbol{s} - \frac{\mathrm{d}\mathbf{u}_D}{\mathrm{d}\boldsymbol{s}} \, \right\|^2_{0,e} \\ \le \widehat{C} \Big\{ \| \, (\boldsymbol{\gamma} - \boldsymbol{\gamma}_h) + \mu(\varphi)^{-1}(\mathbf{u} \otimes \mathbf{u} + \boldsymbol{\sigma})^{\mathtt{d}} - \mu(\varphi_h)^{-1}(\mathbf{u}_h \otimes \mathbf{u}_h + \boldsymbol{\sigma}_h)^{\mathtt{d}} \, \|^2_{0,\Omega} \\ + \sum_{T \in \mathcal{T}_h} h_T^2 \| \, \mathrm{curl} \, \{ \boldsymbol{\gamma}_h + \mu(\varphi_h)^{-1}(\mathbf{u}_h \otimes \mathbf{u}_h + \boldsymbol{\sigma}_h)^{\mathtt{d}} \} \, \|^2_{0,T} \Big\} \\ \le \widetilde{C}_4 \| \, (\vec{\boldsymbol{\sigma}}, \varphi) - (\vec{\boldsymbol{\sigma}}_h, \varphi_h) \, \|^2.$$

□

We recall that, should $\mathbf{u}_D$ not be piecewise polynomial, but smooth enough, we can approximate this data by a Taylor polynomial approximation and the argument just applied would still be valid, with the only difference that higher order terms would appear in the right-hand side of (3.33).

The efficiency bounds for the rest of the terms defining $\boldsymbol{\theta}$ was already considered in [9], where a localization technique based on bubble functions and inverse inequalities is applied, whence we only cite these results next.

Lemma 3.18. *Assume that $\mathbb{K}$ is piecewise polynomial. Then, there exist $\widetilde{C}_5, \widetilde{C}_6 > 0$, independent of h and $\widetilde{h}$, such that*

$$\sum_{T \in \mathcal{T}_h} h_T^2 \| \, \mathrm{div} \, (\mathbb{K} \nabla \varphi_h) - \mathbf{u}_h \cdot \nabla \varphi_h \, \|^2_{0,T} \, \le \, \widetilde{C}_5 \, \| \, (\mathbf{u}, \varphi) - (\mathbf{u}_h, \varphi_h) \, \|^2 \tag{3.46}$$

and

$$\sum_{e \in \mathcal{E}_h(\Omega)} h_e \| \, [\![\mathbb{K} \nabla \varphi_h \cdot \boldsymbol{\nu}]\!] \, \|^2_{0,e} \, \le \, \widetilde{C}_6 \, \| \, (\mathbf{u}, \varphi) - (\mathbf{u}_h, \varphi_h) \, \|^2 . \tag{3.47}$$

Proof. See [9, Lemma 3.18, Lemma 3.19]. □

Lemma 3.19. *Assume that* $\mathbb{K}$ *is piecewise polynomial, that the partition on* Γ *inherited from* $\mathcal{T}_h$ *is quasi-uniform, and that each edge of* $\mathcal{E}_h(\Gamma)$ *is contained in one of the elements of the independent partition of* Γ *defining* $\mathrm{H}^{\lambda}_{\widetilde{h}}$. *Then, there exists* $\widetilde{C}_7 > 0$, *independent of* h *and* $\widetilde{h}$, *such that*

$$\sum_{e\in\mathcal{E}_h(\Gamma)} h_e \| \lambda_{\widetilde{h}} + \mathbb{K}\nabla\varphi_h\cdot\boldsymbol{\nu} \|^2_{0,e} \,\leq\, \widetilde{C}_7 \| (\mathbf{u},\varphi,\lambda) - (\mathbf{u}_h,\varphi_h,\lambda_{\widetilde{h}}) \|^2. \tag{3.48}$$

Proof. See [9, Lemma 3.20]. □

Therefore, the efficiency of the residual-based a posteriori error estimator $\boldsymbol{\theta}$ (cf. Theorem 3.13) is now a consequence of Lemmas 3.15, 3.17, 3.18 and 3.19.

3.4 A fully local estimator

Although being $\boldsymbol{\theta}$ a reliable and efficient estimator, the non-local character of the term $\| \varphi_D - \varphi_h \|^2_{1/2,\Gamma}$ in its definition makes it inadvisable for computational purposes. Instead, we propose the following fully-local a posteriori error estimator:

$$\widetilde{\boldsymbol{\theta}} := \left\{ \sum_{T\in\mathcal{T}_h} \widetilde{\boldsymbol{\theta}}^2_T \right\}^{1/2}, \tag{3.49}$$

where

$$\begin{aligned}
\widetilde{\boldsymbol{\theta}}^2_T := &\, \| \mathbf{e}(\mathbf{u}_h) - \mu(\varphi_h)^{-1}(\mathbf{u}_h\otimes\mathbf{u}_h + \boldsymbol{\sigma}_h)^{\mathtt{d}} \|^2_{0,T} + \| \boldsymbol{\sigma}_h - \boldsymbol{\sigma}_h^{\mathtt{t}} \|^2_{0,T} + \| \boldsymbol{\gamma}_h - \boldsymbol{\omega}(\mathbf{u}_h) \|^2_{0,T} \\
&+ \| \mathbf{div}\,\boldsymbol{\sigma}_h + \varphi_h\mathbf{g} \|^2_{0,T} + h_T^2 \| \mathrm{curl}\,\{\boldsymbol{\gamma}_h + \mu(\varphi_h)^{-1}(\mathbf{u}_h\otimes\mathbf{u}_h + \boldsymbol{\sigma}_h)^{\mathtt{d}}\} \|^2_{0,T} \\
&+ h_T^2 \| \mathrm{div}\,(\mathbb{K}\nabla\varphi_h) - \mathbf{u}_h\cdot\nabla\varphi_h \|^2_{0,T} \\
&+ \sum_{e\in\mathcal{E}_h(T)\cap\mathcal{E}_h(\Omega)} h_e \Big\{ \| [\![\{\boldsymbol{\gamma}_h + \mu(\varphi_h)^{-1}(\mathbf{u}_h\otimes\mathbf{u}_h + \boldsymbol{\sigma}_h)^{\mathtt{d}}\}\boldsymbol{s}]\!] \|^2_{0,e} + \| [\![\mathbb{K}\nabla\varphi_h\cdot\boldsymbol{\nu}]\!] \|^2_{0,e} \Big\} \\
&+ \sum_{e\in\mathcal{E}_h(T)\cap\mathcal{E}_h(\Gamma)} \Big\{ h_e \Big\| \{\boldsymbol{\gamma}_h + \mu(\varphi_h)^{-1}(\mathbf{u}_h\otimes\mathbf{u}_h + \boldsymbol{\sigma}_h)^{\mathtt{d}}\}\boldsymbol{s} - \frac{\mathrm{d}\mathbf{u}_D}{\mathrm{d}\boldsymbol{s}} \Big\|^2_{0,e} \\
&+ h_e \| \lambda_{\widetilde{h}} + \mathbb{K}\nabla\varphi_h\cdot\boldsymbol{\nu} \|^2_{0,e} + \| \mathbf{u}_D - \mathbf{u}_h \|^2_{0,e} + \| \varphi_D - \varphi_h \|^2_{1,e} \Big\}.
\end{aligned} \tag{3.50}$$

Notice that the difference with respect to $\boldsymbol{\theta}$ in (3.1) relies in the last term of (3.50). As in [2, Theorem 4.3] (also in [9, Section 4]), we use interpolation arguments to prove that this estimator is induced by the original one. Indeed, by assuming that $\varphi_D \in \mathrm{H}^1(\Gamma)$ and considering that $\mathrm{H}^{1/2}(\Gamma)$ is the interpolation space between $\mathrm{L}^2(\Gamma)$ and $\mathrm{H}^1(\Gamma)$ with index $1/2$, then there exists $c(\Gamma) > 0$ such that

$$\begin{aligned}
\| \varphi_D - \varphi_h \|^2_{1/2,\Gamma} &\leq c(\Gamma) \| \varphi_D - \varphi_h \|_{0,\Gamma} \| \varphi_D - \varphi_h \|_{1,\Gamma} \\
&\leq c(\Gamma) \| \varphi_D - \varphi_h \|^2_{1,\Gamma} = c(\Gamma) \sum_{e\in\mathcal{E}_h(\Gamma)} \| \varphi_D - \varphi_h \|^2_{1,e}.
\end{aligned} \tag{3.51}$$

Hence, the foregoing argument can be added to what has been developed in Section 3.2 to prove the reliability of this fully-local a posteriori error estimator $\widetilde{\boldsymbol{\theta}}$.

4 Numerical Results

We now present several tests to verify the reliability and efficiency of the fully-local a posteriori error estimator $\boldsymbol{\theta}$, but considering instead the estimator $\widetilde{\boldsymbol{\theta}}$ for the reasons discussed in the previous section. Our implementation is based on a `FreeFem++` code (cf. [18]), the augmented mixed-primal finite element method [1], the Multifrontal Massively Parallel Solver MUMPS (cf. [4]) and the following adaptive algorithm from [20]:

1. Start with a coarse mesh $\mathcal{T}_h$,
2. Solve the discrete problem (2.22) for the current mesh $\mathcal{T}_h$,
3. Compute $\widetilde{\boldsymbol{\theta}}_T$ for each triangle $T \in \mathcal{T}_h$,
4. Check the stopping criteria and decide whether to finish or continue to the next step,
5. Generate an adapted mesh through a variable metric/Delaunay automatic meshing algorithm (see [19, Section 9.1.9]),
6. Define the resulting mesh as $\mathcal{T}_h$ and go to step 2.

We also mention that, should non-zero source terms appear in the right-hand sides of (2.5b) and (2.5c) (let us say, $\mathbf{f}^{\mathtt{m}}$ and $f^{\mathtt{e}}$), some terms in the a posteriori error estimator must be modified. More precisely, the quantities

$$\| \mathbf{div}\, \boldsymbol{\sigma}_h + \varphi_h \mathbf{g} \|_{0,T}^2 \quad \text{and} \quad \| \operatorname{div}(\mathbb{K}\nabla\varphi_h) - \mathbf{u}_h \cdot \nabla\varphi_h \|_{0,T}^2$$

must be replaced by

$$\| \mathbf{div}\, \boldsymbol{\sigma}_h + \varphi_h \mathbf{g} + \mathbf{f}^{\mathtt{m}} \|_{0,T}^2 \quad \text{and} \quad \| \operatorname{div}(\mathbb{K}\nabla\varphi_h) - \mathbf{u}_h \cdot \nabla\varphi_h + f^{\mathtt{e}} \|_{0,T}^2.$$

As usual, we denote the total number of degrees of freedom by DOF, the number of fixed-point iterations by IT, and the error per variable as follows:

$$\begin{aligned} e(\boldsymbol{\sigma}) &:= \| \boldsymbol{\sigma} - \boldsymbol{\sigma}_h \|_{\mathbf{div};\Omega}, & e(\mathbf{u}) &:= \| \mathbf{u} - \mathbf{u}_h \|_{1,\Omega}, & e(p) &:= \| p - p_h \|_{0,\Omega}, \\ e(\boldsymbol{\gamma}) &:= \| \boldsymbol{\gamma} - \boldsymbol{\gamma}_h \|_{0,\Omega}, & e(\varphi) &:= \| \varphi - \varphi_h \|_{1,\Omega}, & e(\lambda) &:= \left\| \lambda - \lambda_{\widetilde{h}} \right\|_{0,\Gamma}. \end{aligned}$$

Then, denoting the total error as

$$e(\vec{\mathbf{t}}) := e(\boldsymbol{\sigma}) + e(\mathbf{u}) + e(\boldsymbol{\gamma}) + e(\varphi) + e(\lambda),$$

we define the experimental rate of convergence of the numerical method and the effectivity index associated to the global estimator $\widetilde{\boldsymbol{\theta}}$ respectively as

$$r(\vec{\mathbf{t}}) := -2\frac{\log(e(\vec{\mathbf{t}})/e'(\vec{\mathbf{t}}))}{\log(\mathrm{DOF}/\mathrm{DOF}')} \quad \text{and} \quad \mathtt{eff}(\widetilde{\boldsymbol{\theta}}) := \frac{e(\vec{\mathbf{t}})}{\widetilde{\boldsymbol{\theta}}},$$

where e and e' denote errors computed on two consecutive meshes of degrees of freedom DOF and DOF$'$.

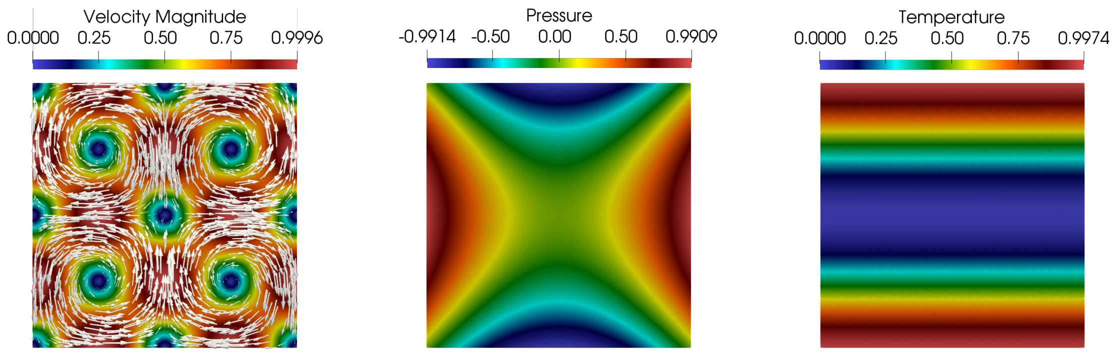

Figure 4.1: Computed solution $(\mathbf{u}_h, p_h, \varphi_h)$ for the data given in Test 1. Results calculated with 746,064 DOF and a second-order approximation $(\mathbb{RT}_1 - \mathbf{P}_2 - P_1 - P_2 - P_1)$.

4.1 Test 1: Accuracy assessment with a smooth solution

For this test, we consider $\Omega := [-1,1]^2$, viscosity, thermal conductivity and body force as

$$\mu(\varphi) = \exp(-0.25\varphi), \quad \mathbb{K} = \mathbb{I}, \quad \mathbf{g} = (0,-1)^{\mathtt{t}},$$

and boundary conditions and source terms such that the exact solution is given by

$$\mathbf{u}(x,y) = \begin{pmatrix} -\cos(\pi x)\sin(\pi y) \\ \sin(\pi x)\cos(\pi y), \end{pmatrix}, \quad p(x,y) = x^2 - y^2, \quad \varphi(x,y) = -0.6944y^4 + 1.6944y^2.$$

In addition, the Korn-like constant and the stabilization parameters are taken as

$$\kappa_0 = 1, \quad \kappa_1 = \frac{\mu_1^2}{\mu_2}, \quad \kappa_2 = \frac{1}{\mu_2}, \quad \kappa_3 = \frac{\kappa_0\mu_1^2}{2\mu_2}, \quad \kappa_4 = \frac{\mu_1^2}{2\mu_2}, \tag{4.1}$$

the viscosity bounds are estimated in $\mu_1 = 0.5$, $\mu_2 = 1.25$, the initial solution for the fixed-point algorithm is taken as $(\mathbf{u},\varphi) = (\mathbf{0}, 0.5)$ and the tolerance is set to 10^{-8}.

We show part of the solution obtained with the present augmented mixed-primal finite element method in Figure 4.1, whereas in Table 4.1 we show the convergence history for a sequence of quasi-uniform mesh refinements and two different orders of approximation. As expected, the rates of convergence of the method when using the elements $\mathbb{RT}_0$ - $\mathbf{P}_1$ - P_0 - P_1 - P_0 and $\mathbb{RT}_1$ - $\mathbf{P}_2$ - P_1 - P_2 - P_1 are $\mathcal{O}(h)$ and $\mathcal{O}(h^2)$, respectively. In addition, the effectivity index $\mathtt{eff}(\widetilde{\boldsymbol{\theta}})$ remains bounded in both cases, thus verifying the reliability of $\widetilde{\boldsymbol{\theta}}$ but also suggesting that this estimator is indeed efficient, as already proved for $\boldsymbol{\theta}$.

4.2 Test 2: Adaptativity in a non-convex domain

Here we consider the L-shaped domain $\Omega := [-1,1]^2 \backslash (0,1)^2$; viscosity, thermal conductivity and body force as

$$\mu(\varphi) = \varphi^{2/3}, \quad \mathbb{K} = \mathbb{I}, \quad \mathbf{g} = (0,1)^{\mathtt{t}},$$

and source terms and boundary conditions as in [15] such that the exact solution is given by

$$\mathbf{u}(x,y) = \begin{pmatrix} -(y-0.1)\big((x-0.1)^2 + (y-0.1)^2\big)^{-1/2} \\ (x-0.1)\big((x-0.1)^2 + (y-0.1)^2\big)^{-1/2}, \end{pmatrix},$$

$$p(x,y) = \frac{1}{x+1.1} + p_0, \quad \varphi(x,y) = \exp\big(0.5x(x-1)y(y-1)\big),$$

Finite Element: $\mathbb{RT}_0$ - $\mathbf{P}_1$ - P_0 - P_1 - P_0					
DOF	$e(\vec{\mathbf{t}})$	$r(\vec{\mathbf{t}})$	$\widetilde{\boldsymbol{\theta}}$	$\texttt{eff}(\widetilde{\boldsymbol{\theta}})$	IT
971	5.6346	-	17.7228	0.3179	10
3,613	2.8609	1.0317	9.6265	0.2972	10
13,781	1.5198	0.9450	5.4870	0.2770	10
54,082	0.7335	1.0656	2.5630	0.2862	10
216,722	0.3807	0.9452	1.3817	0.2755	10
856,008	0.1909	1.0052	0.7082	0.2695	10
$e(\boldsymbol{\sigma})$	$e(\mathbf{u})$	$e(p)$	$e(\boldsymbol{\gamma})$	$e(\varphi)$	$e(\lambda)$
3.5847	2.2294	0.6234	3.7115	0.3538	0.1667
1.7801	0.9826	0.2876	2.0038	0.1734	0.0727
0.8741	0.4811	0.1331	1.1431	0.0827	0.0287
0.4439	0.2406	0.0688	0.5302	0.0426	0.0113
0.2193	0.1193	0.0324	0.2866	0.0211	0.0035
0.1093	0.0586	0.0156	0.1447	0.0105	0.0014

Finite Element: $\mathbb{RT}_1$ - $\mathbf{P}_2$ - P_1 - P_2 - P_1					
DOF	$e(\vec{\mathbf{t}})$	$r(\vec{\mathbf{t}})$	$\widetilde{\boldsymbol{\theta}}$	$\texttt{eff}(\widetilde{\boldsymbol{\theta}})$	IT
3,186	0.6609	0.0000	2.4987	0.2645	10
12,150	0.1643	2.0797	0.6732	0.2441	10
46,950	0.0447	1.9247	0.2015	0.2220	10
185,520	0.0109	2.0520	0.0467	0.2341	10
746,064	0.0029	1.9298	0.0131	0.2181	10
$e(\boldsymbol{\sigma})$	$e(\mathbf{u})$	$e(p)$	$e(\boldsymbol{\gamma})$	$e(\varphi)$	$e(\lambda)$
5.1261e-01	2.8435e-01	1.1166e-01	3.0237e-01	4.0869e-02	7.5810e-03
1.2079e-01	6.5058e-02	2.9820e-02	8.9829e-02	9.6965e-03	3.0753e-03
3.0702e-02	1.6024e-02	7.3302e-03	2.8216e-02	2.2736e-03	9.2860e-04
7.7563e-03	4.1221e-03	1.8236e-03	6.4630e-03	6.0121e-04	2.4973e-04
1.9075e-03	1.0045e-03	4.5206e-04	1.8610e-03	1.4896e-04	6.3515e-05

Table 4.1: Results for Test 1 with a quasi-uniform mesh refinement and two different orders of approximation.

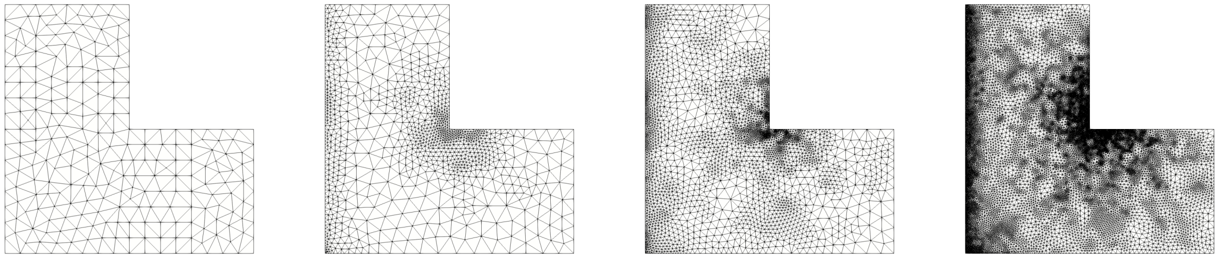

Figure 4.2: From left to right: initial mesh, second, fourth and seventh step of adaptive refinement according to the residual-based a posteriori error estimator $\widetilde{\boldsymbol{\theta}}$ and the data given in Test 2.

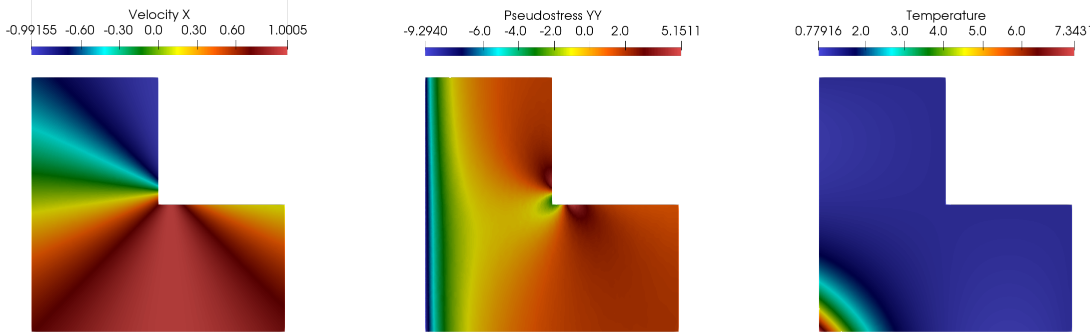

Figure 4.3: Part of the solution to Test 2 (u_1, σ_{22} and φ, respectively the first component of the velocity, fourth component of the pseudostress and temperature) at a seventh step of adaptive refinement (203,779 DOF) with a first order approximation.

where p_0 is a constant such that $p \in L^2_0(\Omega)$, that is, $\int_\Omega p = 0$. Then, the Korn-like constant and the stabilization are taken as in (4.1), the viscosity bounds are estimated in $\mu_1 = 0.5$, $\mu_2 = 4.0$, the initial solution for the fixed-point algorithm is taken as $(\mathbf{u}, \varphi) = (\mathbf{1}, 1)$ and the tolerance is set to 10^{-8}.

As observed from Tables 4.2 and 4.3, in both quasi-uniform and adaptive refinements, the effectivity index remains bounded and the method converges with order $\mathcal{O}(h)$, yet the total error decreases faster in the adaptive scenario, as clearly seen in Figure 4.4, thus lowering the computational cost of computing the solution. In Figure 4.2 we show the resulting meshes at a second, fourth and seventh step of adaptive refinement according to $\widetilde{\boldsymbol{\theta}}$, whereas in Figure 4.3 we show part of the solution to the Boussinesq problem at this last step.

4.3 Test 3: Recovering the optimal rate of convergence

To this end, we consider the *pacman*-shaped domain $\Omega := \{(x, y) : x^2 + y^2 \leq 1\} \backslash (0, 1)^2$. First, we take the viscosity, thermal conductivity and body force as,

$$\mu(\varphi) = \exp(-0.25\varphi) + 0.5, \quad \mathbb{K} = \mathbb{I}, \quad \mathbf{g} := (-\cos(\theta), -\sin(\theta)),$$

then, the boundary conditions and source terms are set such that the exact solution is given by

$$\mathbf{u}(x, y) = \begin{pmatrix} -\cos(\pi x)\sin(\pi y) \\ \sin(\pi x)\cos(\pi y), \end{pmatrix}, \quad p(r, \theta) = -\frac{1}{r^2 - 1.05} + p_0, \quad \varphi(r, \theta) = \frac{0.5}{(r + 0.15)^2},$$

where $r = \sqrt{x^2 + y^2}$, $\theta = \arctan(y/x)$ and p_0 is a constant such that $p \in L^2_0(\Omega)$. Finally, the Korn-like constant and the stabilization parameters are taken as in (4.1), the viscosity bounds are estimated in

DOF	$e(\vec{\mathbf{t}})$	$r(\vec{\mathbf{t}})$	$\widetilde{\boldsymbol{\theta}}$	$\texttt{eff}(\widetilde{\boldsymbol{\theta}})$	IT
2,645	10.8871	-	18.7231	0.5815	10
9,964	6.1331	0.8654	12.0722	0.5080	10
38,814	3.4136	0.8618	8.1652	0.4181	10
153,824	1.8069	0.9240	4.7271	0.3823	10
613,601	0.9013	1.0055	2.3312	0.3866	10
2,440,292	0.4598	0.9752	1.2429	0.3699	10
$e(\boldsymbol{\sigma})$	$e(\mathbf{u})$	$e(p)$	$e(\boldsymbol{\gamma})$	$e(\varphi)$	$e(\lambda)$
8.8244	3.5006	0.8805	3.8140	0.8066	3.6342
5.0580	1.1939	0.4782	2.6564	0.3470	1.8516
2.6700	0.4057	0.2598	1.8729	0.1778	0.9054
1.3629	0.1656	0.1299	1.0862	0.0862	0.4390
0.6885	0.0725	0.0639	0.5332	0.0442	0.2162
0.3411	0.0338	0.0309	0.2862	0.0224	0.1071

Table 4.2: Convergence history for Test 2 with a quasi-uniform refinement and a first order approximation ($\mathbb{RT}_0$ - $\mathbf{P}_1$ - P_0 - P_1 - P_0).

DOF	$e(\vec{\mathbf{t}})$	$r(\vec{\mathbf{t}})$	$\widetilde{\boldsymbol{\theta}}$	$\texttt{eff}(\widetilde{\boldsymbol{\theta}})$	IT
2,645	10.8871	-	18.7231	0.5815	10
5,572	4.8239	2.185	10.7499	0.4487	10
11,494	3.5713	0.8304	7.5754	0.4714	10
20,247	2.6265	1.0855	5.5349	0.4745	10
35,891	1.9149	1.1039	4.2131	0.4545	10
63,390	1.4166	1.0598	3.2468	0.4363	10
113,980	1.0995	0.8637	2.4932	0.4410	10
203,779	0.8085	1.0586	1.8675	0.4329	10
$e(\boldsymbol{\sigma})$	$e(\mathbf{u})$	$e(p)$	$e(\boldsymbol{\gamma})$	$e(\varphi)$	$e(\lambda)$
8.8244	3.5006	0.8805	3.8140	0.8066	3.6342
3.8523	0.6730	0.3861	2.4542	0.3514	1.3529
3.0184	0.4142	0.2882	1.6453	0.3186	0.8146
2.2401	0.2724	0.2309	1.2099	0.2019	0.5490
1.5992	0.1807	0.1630	0.9350	0.1617	0.4200
1.1642	0.1303	0.1220	0.7316	0.1167	0.2926
0.9135	0.0902	0.0923	0.5592	0.0920	0.2127
0.6662	0.0643	0.0683	0.4203	0.0697	0.1553

Table 4.3: Convergence history for Test 2 with an adaptive refinement and a first order approximation ($\mathbb{RT}_0$ - $\mathbf{P}_1$ - P_0 - P_1 - P_0).

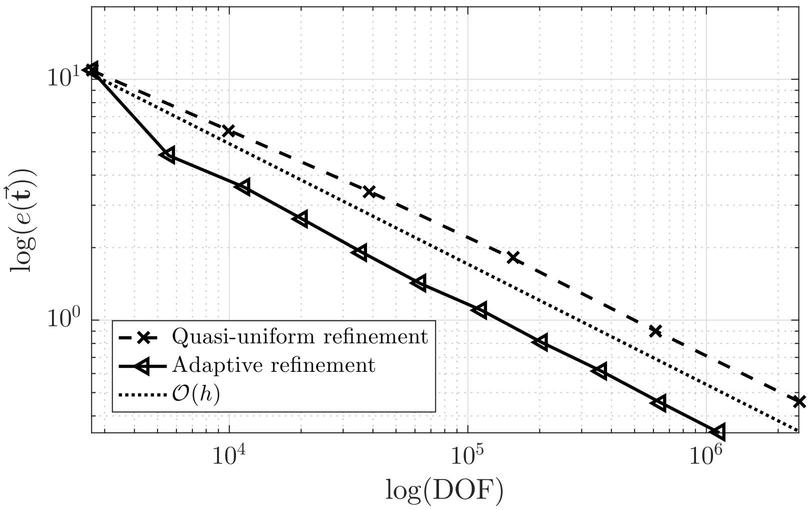

Figure 4.4: Log-log plot of the total error vs. degrees of freedom used with two different refinements for Test 2.

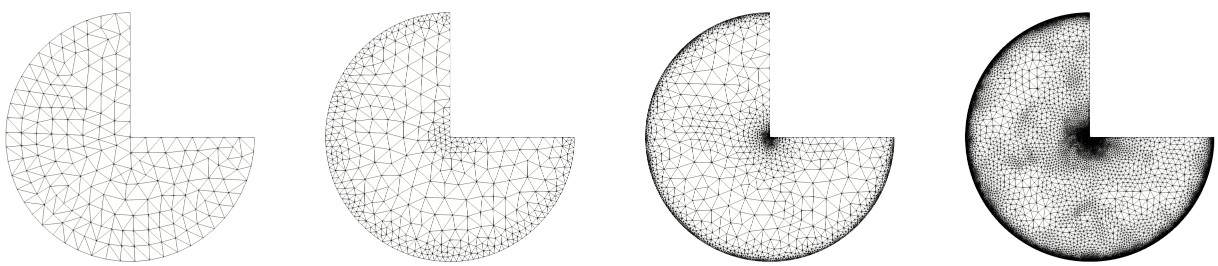

Figure 4.5: From left to right: initial mesh, first, fourth and eighth step of adaptive refinement according to the residual-based a posteriori error estimator $\widetilde{\boldsymbol{\theta}}$ and the data given in Test 3.

$\mu_1 = 0.4$, $\mu_2 = 1.6$, the initial solution for the fixed-point algorithm is taken as $(\mathbf{u}, \varphi) = (\mathbf{0}, 1)$ and the tolerance is also set to 10^{-8}.

In this case, we expect to see some loss in the rate of convergence of the method due to the non-convexity of the domain, as well as from the peculiarities of the exact solution, namely the radial singularity of p in the vicinity of the border, and the high gradient of φ at the origin. This is effectively shown in in Table 4.4, where only a rate of convergence of 0.8 is achieved, however, this can be improved by using an adaptive refinement algorithm that refines the mesh only where it is needed (see Figure 4.5), thus recovering the first order approximation, as shown in Table 4.5 and Figure 4.7. Notice also how the adaptive algorithm improves the efficiency of the method by delivering quality solutions at a lower computational cost, to the point that it is possible to get the same one (in terms of the total error) with only the 7.6% of the DOF of a quasi-uniform mesh. Part of the solution is shown in Figure 4.6 after eight steps of adaptive refinement according to the indicator $\widetilde{\boldsymbol{\theta}}$.

References

[1] J.A. Almonacid, G.N. Gatica and R. Oyarzúa, *A mixed-primal finite element method for the Boussinesq problem with temperature-dependent viscosity*, Preprint 2017-18, Centro de Investigacion en Ingenieria Matematica (CI^{2}MA), Universidad de Concepcion, Chile, (2017).

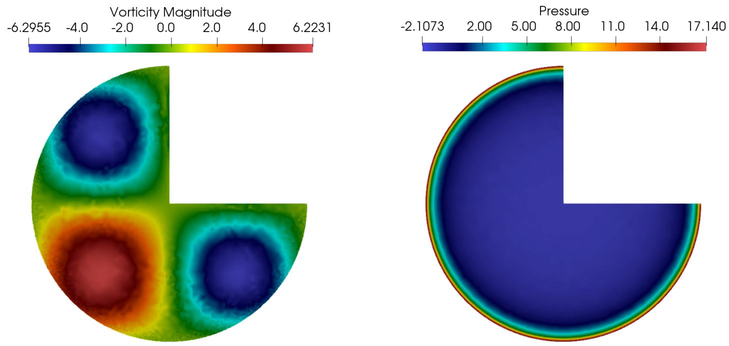

Figure 4.6: Part of the solution to Test 3 at an eighth step of adaptive refinement (153,910 DOF) with a first order approximation.

DOF	$e(\vec{\mathbf{t}})$	$r(\vec{\mathbf{t}})$	$\widetilde{\boldsymbol{\theta}}$	$\mathtt{eff}(\widetilde{\boldsymbol{\theta}})$	IT
2,144	86.8352	-	128.9580	0.6734	10
8,137	76.0434	0.1990	102.4989	0.7419	9
32,817	52.1470	0.5410	82.9869	0.6284	9
127,519	31.9266	0.7229	48.4959	0.6583	9
505,870	18.0019	0.8316	31.0726	0.5794	9
2,029,800	10.2453	0.8113	20.7421	0.4939	9
$e(\boldsymbol{\sigma})$	$e(\mathbf{u})$	$e(p)$	$e(\boldsymbol{\gamma})$	$e(\varphi)$	$e(\lambda)$
82.8051	18.9388	2.8178	7.2408	11.1233	12.1999
73.4766	9.4430	1.8879	5.4210	7.6027	14.4021
50.9156	3.6156	1.0921	3.8405	5.7541	8.1225
29.9066	1.1189	0.5601	2.3001	3.2758	10.3745
15.9038	0.3168	0.2828	1.2420	2.0637	8.0769
8.1100	0.0922	0.1420	0.6587	1.2350	6.1013

Table 4.4: Convergence history for Test 3 with a quasi-uniform refinement and a first order approximation ($\mathbb{RT}_0$ - $\mathbf{P}_1$ - P_0 - P_1 - P_0).

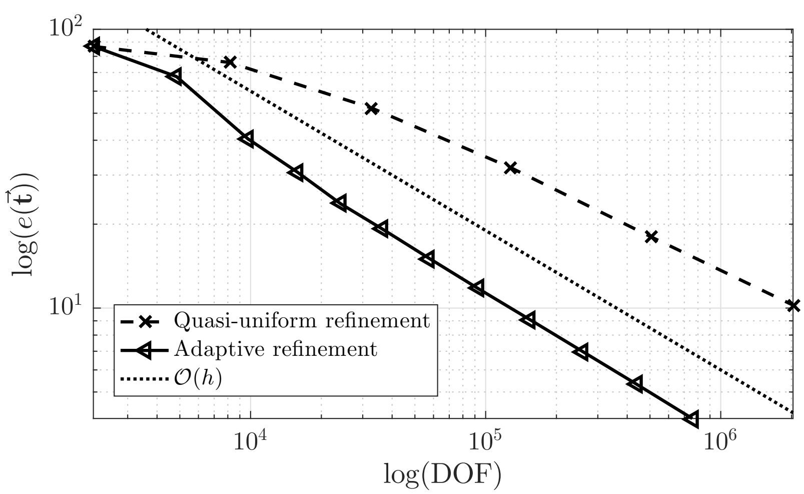

Figure 4.7: Log-log plot of the total error vs. degrees of freedom used with two different refinements for Test 3.

DOF	$e(\vec{\mathbf{t}})$	$r(\vec{\mathbf{t}})$	$\widetilde{\boldsymbol{\theta}}$	$\mathtt{eff}(\widetilde{\boldsymbol{\theta}})$	IT
2,144	86.8352	-	128.9580	0.6734	10
4,840	67.6724	0.6124	91.5469	0.7392	9
9,741	40.4702	1.4701	57.1295	0.7080	9
15,775	30.7849	1.1348	41.0445	0.7500	9
24,181	23.6610	1.2324	30.1959	0.7836	9
36,449	19.1855	1.0219	23.9295	0.8018	9
57,658	15.0588	1.0562	18.6254	0.8085	9
92,874	11.7526	1.0400	14.5601	0.8072	9
153,910	9.0998	1.0129	11.3031	0.8051	9
$e(\boldsymbol{\sigma})$	$e(\mathbf{u})$	$e(p)$	$e(\boldsymbol{\gamma})$	$e(\varphi)$	$e(\lambda)$
82.8051	18.9388	2.8178	7.2408	11.1233	12.1999
66.2496	6.9244	1.5614	2.5628	6.4752	9.7004
39.5461	2.2124	0.9266	2.3256	4.0212	6.8901
30.2017	1.4988	0.7883	2.1479	2.5938	4.6887
23.2207	1.0916	0.6564	1.9609	2.1014	3.3450
18.7641	0.8372	0.5495	1.5096	1.7590	3.1491
14.7031	0.5863	0.4404	1.2981	1.3678	2.5857
11.5017	0.3870	0.3384	1.1054	1.0748	1.8185
8.8862	0.2584	0.2520	0.8937	0.8551	1.4983

Table 4.5: Convergence history for Test 3 with an adaptive refinement and a first order approximation ($\mathbb{RT}_0$ - $\mathbf{P}_1$ - P_0 - P_1 - P_0).

[2] M. Alvarez, G.N. Gatica and R. Ruiz-Baier, *A posteriori error analysis for a viscous flow-transport problem*, ESAIM: Math. Model. Numer. Anal. 50 (2016), no. 6, 1789-1816.

[3] M. Alvarez, G.N. Gatica and R. Ruiz-Baier, *A posteriori error estimation for an augmented mixed-primal method applied to sedimentation-consolidation systems*. Preprint 2016-26, Centro de Investigación en Ingeniería Matemática (CI^{2}MA), Universidad de Concepción, Chile, (2016).

[4] P.R. Amestoy, I.S. Duff and J.-Y. L'Excellent, *Multifrontal parallel distributed symmetric and unsymmetric solvers*, Comput. Methods Appl. Mech. Engrg. 184 (2000), 501-520.

[5] F. Brezzi, and M. Fortin, *Mixed and Hybrid Finite Element Methods*, Springer-Verlag, New York, 1991.

[6] S. Caucao, G.N. Gatica and R. Oyarzúa, *A posteriori error analysis of a fully-mixed formulation for the Navier-Stokes/Darcy coupled problem with nonlinear viscosity*, Comput. Methods Appl. Mech. Engrg. 315 (2017), 943-971.

[7] I.M. Cohen and P.K. Kundu, *Fluid Mechanics*, Third edition. Academic Press, Elsevier, Amsterdam, 2004.

[8] P.G. Clément, *Approximations by finite element functions using local regularization*, RAIRO Modl. Math. Anal. Numér. 9 (1975), 469-484.

[9] E. Colmenares, G.N. Gatica and R. Oyarzúa, *A posteriori error analysis of an augmented mixed-primal formulation for the stationary Boussinesq model*, Calcolo 54 (2017), no. 3, 1055-1095.

[10] E. Colmenares, G.N. Gatica and R. Oyarzúa, *A posteriori error analysis of an augmented fully-mixed formulation for the stationary Boussinesq model.* Preprint 2017-17, Centro de Investigacion en Ingenieria Matematica (CI^{2}MA), Universidad de Concepcion, Chile, (2017).

[11] A. Ern and J-L. Guermond, *Theory and Practice of Finite Elements*, Springer Science & Business Media, New York, 2004.

[12] M. Farhloul, S. Nicaise and L. Paquet, *A refined mixed finite element method for the Boussinesq equations in polygonal domains*, IMA J. Numer. Anal. 21 (2001), no. 2, 525-551.

[13] G.N. Gatica, *A Simple Introduction to the Mixed Finite Element Method: Theory and Applications*, Springer Briefs in Mathematics, Springer, Cham, 2014.

[14] G.N. Gatica and L.F. Gatica, *On the a priori and a posteriori error analysis of a two-fold saddle-point approach for nonlinear incompressible elasticity*, Internat. J. Numer. Methods Engrg 68 (2006), no. 8, 861-892.

[15] G.N. Gatica, L.F. Gatica and A. Márquez, *Augmented mixed finite element methods for a vorticity-based velocity-pressure-stress formulation of the Stokes problem in 2D*, Internat. J. Numer. Methods. Fluids 67 (2011), no. 4, 450-477.

[16] G.N. Gatica, A. Márquez and M.A. Sánchez, *Analysis of a velocity-pressure-pseudostress formulation for the stationary Stokes equations*, Comput. Methods Appl. Mech. Engrg. 199 (2010), no. 17-20, 1064-1079.

[17] G.N. Gatica, R. Ruiz-Baier and G. Tierra, *A posteriori error analysis of an augmented mixed method for the Navier-Stokes equations with nonlinear viscosity*, Comp. Math. Appl. 72 (2016), no.9, 2289-2310.

[18] F. Hecht, *New Development in FreeFem++*, J. Numer. Math. 20 (2012), no. 3-4, 251-265.

[19] F. Hecht, FreeFem++. Third Edition, Version 3.54, `http://www.freefem.org`, (2017).

[20] R. Verfürth, *A Review of A-Posteriori Error Estimation and Adaptive Mesh-Refinement Techniques*, Wiley Teubner, Chichester, 1996.

[21] R. Verfürth, *A Posteriori Error Estimation Techniques for Finite Element Methods*, Numerical Mathematics and Scientific Computation. Oxford University Press, Oxford, 2013.

[22] Y. Zhang, Y. Hou and H. Zuo, *A posteriori error estimation and adaptive computation of conduction convection problems*, Appl. Math. Model. 35 (2011), no. 5, 2336-2347.

Centro de Investigación en Ingeniería Matemática (CI^2MA)

PRE-PUBLICACIONES 2017 - 2018

2017-28 Rodolfo Araya, Manuel Solano, Patrick Vega: *Analysis of an adaptive HDG method for the Brinkman problem*

2017-29 Sergio Caucao, Marco Discacciati, Gabriel N. Gatica, Ricardo Oyarzúa: *A conforming mixed finite element method for the Navier-Stokes/Darcy-Forchheimer coupled problem*

2017-30 Tonatiuh Sanchez-Vizuet, Manuel Solano: *A Hybridizable Discontinuous Galerkin solver for the Grad-Shafranov equation*

2017-31 David Mora, Gonzalo Rivera: *A priori and a posteriori error estimates for a virtual element spectral analysis for the elasticity equations*

2017-32 Gabriel N. Gatica, Mauricio Munar, Filander A. Sequeira: *A mixed virtual element method for a nonlinear Brinkman model of porous media flow*

2018-01 Rodolfo Araya, Ramiro Rebolledo: *An a posteriori error estimator for a LPS method for Navier-Stokes equations*

2018-02 Felipe Lepe, Salim Meddahi, David Mora, Rodolfo Rodríguez: *Mixed discontinuous Galerkin approximation of the elasticity eigenproblem*

2018-03 Marcelo Cavalcanti, Wellington Correa, Mauricio Sepúlveda, Rodrigo Véjar: *Study of stability and conservative numerical methods for a high order nonlinear Schrödinger equation*

2018-04 Julio Aracena, Maximilien Gadouleau, Adrien Richard, Lilian Salinas: *Fixing monotone Boolean networks asynchronously*

2018-05 Ernesto Cáceres, Gabriel N. Gatica, Filander A. Sequeira: *A mixed virtual element method for a pseudostress-based formulation of linear elasticity*

2018-06 Jessika Camaño, Rodolfo Rodríguez, Pablo Venegas: *Convergence of a lowest-order finite element method for the transmission eigenvalue problem*

2018-07 Javier A. Almonacid, Gabriel N. Gatica, Ricardo Oyarzúa: *A posteriori error analysis of a mixed-primal finite element method for the Boussinesq problem with temperature-dependant viscosity*

Para obtener copias de las Pre-Publicaciones, escribir o llamar a: Director, Centro de Investigación en Ingeniería Matemática, Universidad de Concepción, Casilla 160-C, Concepción, Chile, Tel.: 41-2661324, o bien, visitar la página web del centro: http://www.ci2ma.udec.cl

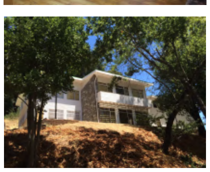

CENTRO DE INVESTIGACIÓN EN
INGENIERÍA MATEMÁTICA (CI^2MA)
Universidad de Concepción

Casilla 160-C, Concepción, Chile
Tel.: 56-41-2661324/2661554/2661316
http://www.ci2ma.udec.cl